NASA/TP—2013–218036

Effectiveness of a Wedge Probe to Measure Sonic Boom Signatures in a Supersonic Wind Tunnel

Floyd J. Wilcox, Jr., and Alaa A. Elmiligui
Langley Research Center, Hampton, Virginia

August 2013

NASA STI Program . . . in Profile

Since its founding, NASA has been dedicated to the advancement of aeronautics and space science. The NASA scientific and technical information (STI) program plays a key part in helping NASA maintain this important role.

The NASA STI program operates under the auspices of the Agency Chief Information Officer. It collects, organizes, provides for archiving, and disseminates NASA's STI. The NASA STI program provides access to the NASA Aeronautics and Space Database and its public interface, the NASA Technical Report Server, thus providing one of the largest collections of aeronautical and space science STI in the world. Results are published in both non-NASA channels and by NASA in the NASA STI Report Series, which includes the following report types:

- TECHNICAL PUBLICATION. Reports of completed research or a major significant phase of research that present the results of NASA Programs and include extensive data or theoretical analysis. Includes compilations of significant scientific and technical data and information deemed to be of continuing reference value. NASA counterpart of peer-reviewed formal professional papers, but having less stringent limitations on manuscript length and extent of graphic presentations.

- TECHNICAL MEMORANDUM. Scientific and technical findings that are preliminary or of specialized interest, e.g., quick release reports, working papers, and bibliographies that contain minimal annotation. Does not contain extensive analysis.

- CONTRACTOR REPORT. Scientific and technical findings by NASA-sponsored contractors and grantees.

- CONFERENCE PUBLICATION. Collected papers from scientific and technical conferences, symposia, seminars, or other meetings sponsored or co-sponsored by NASA.

- SPECIAL PUBLICATION. Scientific, technical, or historical information from NASA programs, projects, and missions, often concerned with subjects having substantial public interest.

- TECHNICAL TRANSLATION. English-language translations of foreign scientific and technical material pertinent to NASA's mission.

Specialized services also include organizing and publishing research results, distributing specialized research announcements and feeds, providing information desk and personal search support, and enabling data exchange services.

For more information about the NASA STI program, see the following:

- Access the NASA STI program home page at *http://www.sti.nasa.gov*

- E-mail your question to help@sti.nasa.gov

- Fax your question to the NASA STI Information Desk at 443-757-5803

- Phone the NASA STI Information Desk at 443-757-5802

- Write to:
  STI Information Desk
  NASA Center for AeroSpace Information
  7115 Standard Drive
  Hanover, MD 21076-1320

NASA/TP—2013–218036

Effectiveness of a Wedge Probe to Measure Sonic Boom Signatures in a Supersonic Wind Tunnel

Floyd J. Wilcox, Jr., and Alaa A. Elmiligui
Langley Research Center, Hampton, Virginia

National Aeronautics and
Space Administration

Langley Research Center
Hampton, Virginia 23681–2199

August 2013

Level of review: This material has been technically reviewed by a committee of peers.

Available from:

NASA Center for AeroSpace Information
7115 Standard Drive
Hanover, MD 21076–1320
443-757-5802

Summary

A wind tunnel investigation was conducted in the Langley Unitary Plan Wind Tunnel (UPWT) to determine the effectiveness of a wedge probe to measure sonic boom pressure signatures. A generic business jet model at a constant angle of attack and at a single model to probe separation distance was used to generate a sonic boom signature. Sonic boom pressure signatures were acquired with both a wedge probe and a slender conical probe for comparison. The test was conducted at a Mach number of 2.0 and a free-stream unit Reynolds number of 2 million per foot. The results showed that the wedge probe was not effective in measuring the sonic boom pressure signature of the aircraft model because the spatial separation of three measured pressures on the wedge probe violated an assumption in the development of the wedge probe data reduction equations that the entire probe is in a uniform flow field.

Introduction

Experimental research to measure sonic boom pressure signatures of aircraft in wind tunnels has been conducted since the 1950s using a variety of techniques (ref. 1–9). Through the years, the technique that used slender conical probes became the predominate standard for measuring sonic boom pressure signatures. Because slender conical probes only measure local static pressure, reference 10 described the development of a wedge probe that could not only determine local static pressure but also stagnation pressure, Mach number, and flow angularity in the flow field of an aircraft. Reference 10 presented the results of a wind tunnel test using the wedge probe and stated that the probe worked well in the free-stream flow; however, wind tunnel problems during the test prevented the acquisition of sonic boom pressure signatures of an aircraft model. In the late 2000s, another similar but larger wedge probe was fabricated and tested in both a wind tunnel and in flight as described in reference 11. The wind tunnel test of the second wedge probe did not measure the sonic boom signature of an aircraft model but rather measured the pressure signature created by a disturbance bump mounted to the tunnel sidewall. To date, the sonic boom signature of an aircraft model has not been measured in a wind tunnel using a wedge probe. In the present study, a wind tunnel test was conducted to investigate the effectiveness of a wedge probe to measure sonic boom pressure signatures.

A wind tunnel investigation was performed in the Langley Unitary Plan Wind Tunnel (UPWT) to measure the sonic boom pressure signature of an aircraft model using both the wedge probe described in reference 11 and a slender conical probe for comparison. The sonic boom pressure signature was generated with an existing generic business jet model. The investigation was conducted as part of a wind tunnel test that studied the ability of a slender conical probe to measure sonic boom signatures while continuously moving the aircraft model past the probe as described in reference 12. The tests were conducted at a Mach number of 2.0 and at a free-stream unit Reynolds number of 2 million per foot. The sonic boom pressure signatures were obtained with the model at a single angle of attack ($\approx 2.3°$) and at a model nose to survey probe (wedge or slender conical) separation distance of 13.5 in.

Nomenclature

Abbreviations and Acronyms

AOA	angle of attack, deg
ID	inside diameter
NF	normal force, lbf

OD	outside diameter
PM	pitching moment, in·lbf
PRT	platinum resistance thermometer
psfa	pound-force per square foot absolute (lbf/ft^2)
psfd	pound-force per square foot differential (lbf/ft^2)
SLSLE	straight-line segmented leading edge
UPWT	Unitary Plan Wind Tunnel

Symbols

h	distance from model nose to survey probe (wedge or conical) measured perpendicular to tunnel sidewall (see figure 2b and 4c), in.
M	Mach number
p	free-stream static pressure, psfa
p_0	free-stream stagnation pressure, psfa
p_{03}	measured stagnation pressure behind normal shock on wedge probe upper surface (see figure A1), psfa
p_{04}	measured stagnation pressure ahead of wedge probe oblique shock and behind normal shock (see figure A1), psfa
p_1	computed static pressure ahead of wedge probe (see figure A1), psfa
p_{ref}	reference probe pressure, psfa
q	free-stream dynamic pressure, psfa
Re	free-stream unit Reynolds number $\times 10^{-6}$, ft^{-1}
T_0	free-stream stagnation temperature, °F
v	aircraft model longitudinal speed during continuous sweep runs, in/s
α	angle of attack, deg
Δp	measured differential pressure between survey probe and reference probe or the differential between the computed static pressure ahead of the wedge probe and the measured reference probe pressure $(p_1 - p_{ref})$, psfd
$(\Delta p/p_{ref})_{avg}$	average sonic boom pressure signature parameter where $\Delta x \leq 21.25$ in.
$(\Delta p/p_{ref})_{cor}$	corrected sonic boom pressure signature parameter (see equation 1)
$(\Delta p/p_{ref})_{unc}$	uncorrected sonic boom pressure signature parameter
Δx	distance from model nose to survey probe orifices or wedge probe leading edge measured parallel to tunnel sidewall (see figure 2b and 4c), in.
γ	ratio of specific heats

Apparatus and Experimental Methods

Wind Tunnel Description

The wind tunnel test was conducted in the Langley Unitary Plan Wind Tunnel, which is a continuous flow, variable pressure, supersonic wind tunnel. The tunnel contains two test sections that are approximately 4 ft by 4 ft square and 7 ft long. Each test section covers only part of the Mach number range of the tunnel. The nozzle ahead of each test section consists of an asymmetric sliding block that allows continuous Mach number variation during tunnel operations from 1.5 to 2.9 in the low Mach number test section (#1) and 2.3 to 4.6 in the high Mach number test section (#2). Reference 13 contains a complete description of the facility along with test section calibration information.

Table 1 shows the nominal free-stream conditions used during this investigation in test section #1. Test section #2 was not used for this test.

Table 1. Nominal free-stream test conditions

M	Re, ft^{-1}	p_0, psfa	T_0, °F	q, psfa	p, psfa
2.00	2.00	1253	125	448.5	160.2

The tunnel air dew point was maintained below −20°F (at atmospheric pressure) to minimize water vapor condensation effects.

General Test Description

Conical Survey Probe

Figure 1 shows a photograph and sketch of the wind tunnel test setup for the slender conical survey probe. One of the test section doors that normally contains schlieren windows was replaced with a solid steel door so that some of the sonic boom measurement hardware (free-stream reference probe, survey probe, and transducer box) could be attached to the tunnel sidewall. The reference probe, which was also a slender conical probe, was mounted to the tunnel sidewall above and slightly upstream of the survey probe using a fixed (nonmovable) support bracket. The conical survey probe was mounted to the sidewall near the tunnel centerline using a support that was part of a mechanism that could move the probe longitudinally in the test section. However, during this test the conical survey probe remained at a fixed longitudinal position for all runs where it was used. A transducer box was located above and downstream of the conical survey probe location and was used to house pressure transducers that measured the differential pressure between the reference and survey probes, and a transducer that measured just the reference probe pressure. Figure 2 shows the relative positions of the sonic boom hardware. Figure 3 shows the overall dimensions of the reference probe mounting bracket, survey probe mechanism, and transducer box. Details of the reference and survey probes are presented in the Instrumentation and Measurements section.

Wedge Survey Probe

Figure 4 shows a photograph and sketch of the wind tunnel test setup for the wedge survey probe. The test layout for the wedge survey probe was exactly the same as the conical survey probe except that the conical survey probe and mechanism were replaced by the wedge probe and a wedge probe holder. The leading edge of the wedge survey probe at the probe centerline was located at the same position in the tunnel as the pressure orifices in the conical survey probe. The reference probe remained on the tunnel sidewall, and the measured reference probe pressure was used in the wedge survey probe data reduction similar to the conical survey probe data reduction (see Corrections section). Figure 5 shows the overall dimensions of the wedge probe holder. Details of the wedge survey probe are presented in the Instrumentation and Measurements section.

Aircraft Model

The aircraft model used during this test was a generic business jet configuration that had previously been tested in UPWT and was designated as the straight-line segmented leading edge (SLSLE) model. A sketch and photograph of the model are shown in figure 6. The SLSLE model was chosen for this test because it was available and because data from the previous test were accessible for comparison (ref. 8). The SLSLE model was tested without boundary layer transition grit. The SLSLE configuration was designed using the following criteria:

- Cruise Mach number 2.00
- Beginning cruise weight .... 88,000 lbf
- Beginning cruise altitude .... 53,000 ft
- Sonic boom ground overpressure .... 0.5 psfd

Additional details about the overall design of the model can be found in references 8 and 14.

Model Installation

The SLSLE model and sting were pinned together and were designed not to be taken apart. The sting was attached to the sonic boom angle of attack (AOA) mechanism, which was in turn attached to the tunnel roll coupling and model support system (see fig. 1a). The SLSLE model was tested with positive normal force in the horizontal plane, i.e., wings vertical, for all of the sonic boom pressure signature runs.

The tunnel angle of attack mechanism was not used to set the model angle of attack and remained at a fixed position during this test. Instead, the sonic boom AOA mechanism was used to set the model angle of attack to approximately 2.3°. The AOA consisted of both the pitch angle set with the sonic boom AOA mechanism and deflection caused by aerodynamic loads. During this test, the sonic boom AOA mechanism pitch angle was set to approximately 1.7° to match one of the settings used during the previous test of the SLSLE model in UPWT. Because data from a previous test that used the sonic boom AOA mechanism showed that the mechanism contained approximately 0.2° of play (movement of the pitch mechanism that was not indicated by a linear potentiometer located inside the mechanism), a jam nut was fabricated and installed in the mechanism to lock it at the required pitch angle. Figure 7 shows the jam nut installed in the sonic boom AOA mechanism.

The tunnel model support system was used to position the SLSLE model laterally and longitudinally in the test section relative to the conical probe or the wedge probe. During this test, the model nose was positioned at $h \approx 13.5$ in. (see fig. 2b and 4c) then the tunnel model support system was disabled in the lateral direction to prevent h from varying during the test. The tunnel model support system longitudinal movement capability was used to move the SLSLE model past either the conical probe or wedge probe to measure the sonic boom pressure signature. During each pressure signature run, the model was moved longitudinally approximately 16.5 in.

During a typical run, the SLSLE model was initially positioned so that the nose shock was located downstream of the conical survey probe or wedge probe. The model was moved forward in 0.125 in. increments while the model sonic boom pressure signature data were acquired. Wedge probe data were also acquired in continuous sweep runs where the model was moved continuously past the probe. During the continuous sweep runs, the model was again positioned so that the nose shock was located downstream of the wedge probe. The data acquisition system was started, and approximately 10 s of data were acquired before the model movement began. After the model was moved forward the required distance, the model movement was stopped, and data were acquired for an additional 10 s.

Instrumentation and Measurements

Sketches of the conical reference and survey probes are shown in figure 8. The probes were identical 4° included angle cones with a hole drilled through the probe and into a central chamber creating two static pressure orifices. For these tests, the free-stream reference probe orifices were oriented such that one orifice was on top of the probe and the other on the bottom of the probe when viewing the probe from the side, i.e., looking into the tunnel sidewall. The conical survey probe orifices should have been oriented the same as the reference probe; however, because of an installation mistake, they were oriented such that one orifice was facing the tunnel sidewall used to mount the probes and the other was facing toward the model. Comparison of the sonic boom pressure signatures from the current test to a signature obtained during the previous test of the same model in UPWT shows no significant differences indicating that the misalignment of the conical survey probe orifices did not adversely affect the pressure signature. The comparison will be presented later in this report. The lengths of stainless steel tubing used to connect the reference and survey probes to the pressure transducers located in the transducer box are noted in figure 8. The final pressure connections inside the transducer box used flexible tubing (7/32 in. outside diameter, OD, by 3/32 in. inside diameter, ID).

Figure 9 shows a schematic of the reference and conical survey probe connections to the pressure transducers. A solenoid activated valve that could be remotely operated was used to equalize the pressures across the differential pressure transducer to minimize the risk of over pressurizing the transducer during tunnel start and stops. The differential pressure between the reference and conical survey probe was measured with a ±13.006 psfd (±2.5 in. water column) pressure transducer, which had a quoted accuracy of ±0.018 psfd in the manufacturer's product literature. An in-situ calibration of the differential pressure transducer was performed, and the uncertainty in the difference between the applied and measured pressures, otherwise know as the regression uncertainty, was ±0.016 psfd at a 95 % confidence level. In addition, the reference probe pressure was measured directly with a 720 psfa absolute pressure transducer, which had a manufacturer's quoted accuracy of ±0.72 psfa. An in-situ calibration of the absolute pressure transducer was performed, and the regression uncertainty was ±0.172 psfa at a 95 % confidence level.

The transducer box was located on the tunnel sidewall above and downstream of the reference and conical survey probes. The purpose of the transducer box was to house the differential and absolute pressure transducers as close to the reference and conical survey probes as possible to minimize pressure lag effects. The transducer box was sealed, and the inside was maintained at near atmospheric conditions so that there would be no significant temperature or pressure effects on the pressure transducers. The solenoid activated valve was also located inside the transducer box. Figure 10 shows the inside of the transducer box with the two pressure transducers and solenoid valve.

The transducer box was fabricated out of aluminum with a polycarbonate insulating cover, which can be seen in figure 1a. The aluminum box was water cooled using 0.125 in. OD copper tubing epoxied into grooves machined into the sides, top, and bottom of the box. There were four separate cooling circuits for the left side, right side, top, and bottom of the transducer box. Cooling water was supplied to each circuit, and the water flow was controlled with a small brass needle valve. In addition to the water cooling, atmospheric air was circulated inside the box to help maintain a constant temperature inside the box. Two 0.5 in. OD nylon tubes were routed to the box and were used to supply cooling air to the box using a vacuum cleaner to pull atmospheric air through one of the nylon tubes, into the box, and then out the second nylon tube. Six type T (copper/copper-nickel) thermocouples were installed inside the transducer box to monitor the differential pressure transducer, air, and transducer box wall temperatures.

Sketches and photographs of the wedge probe are shown in figure 11. The wedge probe had a half angle of 8°. The upper surface of the wedge probe had a total pressure tube and two static pressure orifices (teed together) in the wedge surface. The lower wedge surface had a single total pressure tube. Three pressure transducers were located inside the cylindrical portion of the wedge probe. The total pressure tubes were measured with individual 10 psia transducers, and the static pressure orifices were measured with a 5 psia transducer. The manufacturer's quoted accuracies of the 10 psia and 5 psia transducers were ±0.05 psia and ±0.025 psia, respectively.

A type T thermocouple was attached to the aft end of the cylindrical portion of the wedge probe near the electrical connector as shown in figure 12. For this photograph, the cover plate on the wedge probe holder was removed, and the wedge probe was positioned further downstream in the holder than the normal wind on position. The purpose of this thermocouple was to measure the approximate temperature of the pressure transducers during the wind-on runs. The pressure transducers were supposed to be temperature compensated; however, previous calibrations of the transducers at NASA Dryden Flight Research Center showed that some of the transducers were not well temperature compensated (ref. 11). Therefore, the pressure transducers were recalibrated after the present test at the approximate mean temperature measured by the thermocouple during all wedge probe runs (95°F). All of the wedge probe data were re-reduced after the test using the new pressure transducer calibration constants.

Normal force and pitching moment data on the SLSLE model were measured with a 2-component electrical strain gage balance that was integral to the sting. The strain gages were located near the aft end of the sting and were covered with auto body filler that was faired to the sting contour. Figure 13 shows the locations of the model and balance moment reference centers. The full scale balance limits are shown in table 2 along with the computed balance accuracies as a percentage of full scale balance limits. To compute the balance accuracies, the balance calibration data were run through the balance calibration equations. The standard deviation of the difference between the computed and applied loads was determined for all of the calibration loads. The balance accuracies reported in table 2 are at a 95 % confidence level.

Table 2. Range and accuracy of balance components

Component	Range	Accuracy
Normal force	±5 lbf	±0.23 % of full scale
Pitching moment	±109.2 in·lbf	±0.04 % of full scale

Two platinum resistance thermometers (PRT) were installed on the sting; one near the forward balance bridge and the second near the aft balance bridge. The purpose of the PRTs was to monitor the temperature gradient across the balance bridges and not to compensate for balance sensitivity changes caused by temperature. Data were only acquired after the two PRT temperatures stabilized with minimal temperature differential.

The tunnel stagnation pressure was measured with a 100 psia bourdon tube pressure transducer that had a manufacturer's quoted accuracy of ±0.003 psia at a 95 % confidence level. The tunnel stagnation temperature was measured with a platinum resistance thermometer.

The model support system lateral and longitudinal movement were measured by absolute rotary encoders that were mounted to the system drive screws. The estimated accuracy of the model support system position based on calibration data was ±0.005 in. for both the longitudinal and lateral positions.

The model support system AOA was measured with an accelerometer mounted to the support system just downstream of the roll coupling and was adjusted so that the sonic boom AOA mechanism was level before the SLSLE model was rolled to the wings vertical position. The model support AOA mechanism was not adjusted after leveling the sonic boom AOA mechanism.

The sonic boom AOA mechanism pitch angle was measured with a linear potentiometer. As discussed earlier, a jam nut was used to lock the mechanism to a single pitch angle. However, the jam nut could have locked in some unknown pitch error caused by the sonic boom AOA mechanism play. Based on unpublished checks conducted during a previous test, the mechanism play (and, consequently, the unknown pitch error) was as large as 0.2°. Because the sonic boom AOA reading probably contained some fixed unknown error, the computed SLSLE model nose separation distance, h, which was a function of the pitch angle, also probably contained some error. However, since the pitch angle was fixed for the entire test, the small error in h would be constant for the entire test and, therefore, would not affect the results or conclusions of the test.

Data were acquired in either a move-pause or continuous mode depending on the run. The data acquisition system scan rate for the move-pause runs was 30 frames/s for two seconds; all of the instrumentation readings (millivolt values) acquired during the two second period were averaged before data reduction. The data acquisition system scan rate for the continuous runs was 120 frames/s. The data acquisition system used a 1 Hz low pass filter (2-pole Butterworth).

Wedge Probe Data Reduction

Using the two stagnation pressure measurements and the upper surface static pressure measurement on the wedge probe, an iterative procedure as described by Bobbitt (ref. 10 and 11) can determine the static pressure ahead of the wedge probe. The step by step procedure used for the wedge probe data obtained during this test is documented in the appendix. The computed static pressure ahead of the wedge probe is then used to compute the sonic boom pressure signature parameter.

Corrections

The data acquired during the test were not corrected for tunnel flow angularity. The distance from the model nose to the conical survey probe or wedge probe measured perpendicular to tunnel sidewall, h, was corrected for sting deflection caused by aerodynamic loads. In addition, the model AOA was corrected for sting deflection caused by aerodynamic loads. Because the sonic boom AOA mechanism was locked at one position, the SLSLE model AOA remained at approximately 2.3° for the entire test.

The measured sonic boom pressure signature parameter was defined as $(\Delta p/p_{ref})_{unc}$. For the conical survey probe, Δp was the measured differential pressure between the conical survey probe and the reference probe. For the wedge survey probe, Δp was the difference between the computed static pressure ahead of the wedge probe and the reference probe pressure $(p_1 - p_{ref})$.

Because of static pressure variation within the tunnel test section, the Δp values for the conical and wedge survey probes were not equal to zero. Consequently, the uncorrected sonic boom pressure signature parameter, $(\Delta p/p_{ref})_{unc}$, was also not equal to zero when the model nose shock was located downstream of either the conical survey probe or wedge survey probe, i.e., the probes were located in the free-stream flow. Therefore, the sonic boom pressure signatures were adjusted by averaging all $(\Delta p/p_{ref})_{unc}$ values with $\Delta x \leq 21.25$ in. during a signature run (conical and wedge survey probes located in the free-stream flow) and subtracting the average value from each

$(\Delta p/p_{ref})_{unc}$ value, i.e.,

$$\left(\frac{\Delta p}{p_{ref}}\right)_{cor} = \left(\frac{\Delta p}{p_{ref}}\right)_{unc} - \left(\frac{\Delta p}{p_{ref}}\right)_{avg} \tag{1}$$

Figure 14 shows typical corrected and uncorrected sonic boom pressure signatures as a function of Δx for the conical and wedge survey probes to illustrate the approximate magnitude of the correction. No additional corrections or adjustments were performed to the sonic boom pressure signature data.

Results and Discussion

All of the plots in this section will show the corrected sonic boom pressure signature parameter $(\Delta p/p_{ref})_{cor}$ as a function of Δx. As mentioned previously, the sonic boom angle of attack mechanism was locked at one position to eliminate inadvertent angle of attack changes caused by the play in the mechanism. The resultant angle of attack of the SLSLE model was approximately 2.3° for the entire test.

Conical Survey Probe Data Comparison Between Tests

Figure 15 shows a comparison between the sonic boom pressure signature data as a function Δx for two sets of three back-to-back repeat runs obtained during the current test and data acquired during the previous test of this model in UPWT as described in reference 8. The two sets of back-to-back repeat runs were obtained on two different days. The results show reasonable agreement between the six repeat runs of the current test. Comparison with the previous test data shows a slight (≈ 0.5 in.) positive shift in Δx for the previous data. However, the magnitude and location of the signature peaks compare well between the tests indicating that nothing significant had changed between the tests, which gave confidence that the current test setup was satisfactory. The cause of the Δx shift between the two tests is unknown.

One significant difference between the tests is apparent near $\Delta x = 33$ in. The previous test data show a negative peak as the flow expands aft of the model wing whereas the data for the current test flattens and does not peak. For the current test, the differential pressure transducer that measured Δp was over scaled in this region, and an internal mechanical stop inside the transducer prevented over pressurization of the transducer. Although most details of the previous and current test were identical, the reference and survey probes for the previous test were 2° included angle cones while the current test used probes with 4° included angles. The larger angles on the reference and survey probes resulted in a larger measured Δp that caused the differential pressure transducer diaphragm to hit the mechanical stop resulting in a constant millivolt output from the transducer. Because the purpose of this test was to compare the conical survey probe data with the wedge survey probe data, the over pressurization of the differential pressure transducer in this region did not affect the conclusions of this test.

Data Comparison Between Conical and Wedge Survey Probes

Figure 16 shows comparisons between the sonic boom pressure signatures obtained with the conical probe and the wedge probe. Two sets of three back-to-back runs were obtained on two different days for both the conical probe and the wedge probe. Each set of repeat runs are shown in figure 16. The results show that the wedge probe signatures are offset in the $+\Delta x$ direction relative to the conical probe data and that the magnitude of the signature peaks were generally larger than the conical probe data.

At the beginning of the pressure signatures, the sonic boom pressure signature parameter is zero for both the conical probe and wedge probe because the model nose shock is downstream of both the conical and wedge probes. At $\Delta x \lesssim 22$ in., the wedge probe pressure signature shows a significant decrease while the conical probe signature is still zero. The reason for the sharp decrease in the wedge probe signature is illustrated in figure 17. At the beginning of the wedge probe pressure signature, the model nose shock is downstream of the wedge probe and, consequently, the wedge probe is located in the free-stream flow. As the pressure signature run progresses, the nose shock will eventually pass over the wedge upper surface stagnation pressure tube (p_{03}), but the upper wedge surface static pressures (p_2) and lower surface stagnation pressure tube (p_{04}) will be upstream of the model nose shock. Because the equations used to calculate the wedge probe parameters were derived assuming the entire probe is in a uniform flow field, the spatial separation of the pressure measurements on the wedge probe results in an incorrect calculation of the static pressure ahead of the wedge probe, p_1. Because the wedge probe is never located in a uniform flow field along the entire sonic boom pressure signature (except at the beginning of the signature), the entire wedge probe signature is affected by the pressure measurement spatial separation issue.

To better illustrate the wedge probe pressure measurement spatial separation issue, the wedge probe individual pressure measurements that were obtained during a continuous run were plotted. Details of acquiring continuous sonic boom pressure signature data are given in reference 12. During the continuous run, the SLSLE model was continuously moved in the axial direction while the pressure signature data were obtained. Figure 18 shows a comparison between the wedge probe move-pause pressure signatures from figure 16a compared to a single continuous pressure signature obtained with the wedge probe. The continuous wedge probe pressure signature is similar to the move-pause data except that the continuous data shows more unsteadiness because the continuous data were not averaged. Figure 19 shows a comparison between the slender conical probe move-pause pressure signatures from figure 16a compared to the single continuous pressure signature obtained with the wedge probe that is shown in figure 18. Finally, figure 20 shows the continuous data individual wedge probe pressures from figure 19 plotted as function of Δx for values near 22 in., i.e., the Δx location where the model nose shock first passes over the wedge probe. The thick vertical lines on the plots for p_{03}, p_2, and p_{04} show approximately where the pressures begin to rise as the nose shock passes over each of the pressure orifices or tubes. The plot of p_1, which is computed from the wedge probe equations, shows that p_1 remains constant at approximately 160 psfa while the model nose shock is downstream of the wedge probe. As the nose shock passes over the upper surface stagnation pressure tube, p_{03} increases and p_1 begins to decrease, which causes $(\Delta p/p_{ref})_{cor}$ to decrease as previously shown in figure 19.

Although it is possible to reduce the size of the wedge probe and, thus, reduce the spatial separation of the probe pressure measurements as suggested in reference 10, there will always be spatial separation of the pressure measurements that will cause issues measuring sonic boom pressure signatures with the wedge probe in supersonic wind tunnels.

Concluding Remarks

A wind tunnel investigation was conducted in the Langley Unitary Plan Wind Tunnel to determine the effectiveness of a wedge probe to measure aircraft sonic boom signatures compared to slender conical probes, which have typically been used in the past. Sonic boom signatures were measured on an existing generic business jet model at a constant angle of attack and at a model nose to survey probe (wedge or conical) separation distance of 13.5 in. The sonic boom signatures were obtained at a Mach number of 2.0 and at a free-stream unit Reynolds number of 2 million per foot.

The results of the test showed significant differences between the sonic boom pressure signatures measured with the wedge probe compared to the conical probe. The wedge probe data reduction equations assumed that the probe was located in a uniform flow field, and the spatial separation of three measured pressures on the wedge probe caused the calculation of the static pressure ahead of the wedge probe to be in error. Because the wedge probe is never located in a uniform flow field along the entire sonic boom pressure signature (except at the beginning of the signature), the entire wedge probe signature is affected by pressure measurement spatial separation issue. Although it is possible to reduce the size of the wedge probe and, thus, reduce the spatial separation of the probe pressure measurements, there will always be spatial separation of the pressure measurements that will cause issues measuring sonic boom pressure signatures with the wedge probe in supersonic wind tunnels.

References

1. Carlson, Harry W.: *An Investigation of Some Aspects of the Sonic Boom by Means of Wind-Tunnel Measurements of Pressures about Several Bodies at a Mach Number of 2.01.* NASA TN D–161, 1959.

2. Carlson, Harry W.: *Correlation of Sonic-Boom Theory with Wind-Tunnel and Flight Measurements.* NASA TR R–213, 1964.

3. Mendoza, Joel P.; and Hicks, Raymond M.: *Further Studies of the Extrapolation of Near-Field Overpressure Data.* NASA TM X–2219, 1971.

4. Hunton, Lynn W.; Hicks, Raymond M.; and Mendoza, Joel P.: *Some Effects of Wing Planform on Sonic Boom.* NASA TN D–7160, 1973.

5. Carlson, H. W.; and Morris, O. A.: Wind-Tunnel Sonic-Boom Testing Techniques. AIAA Paper 66–765, 1966.

6. Carlson, Harry W.; Mack, Robert J.; and Morris, Odell A.: *A Wind-Tunnel Investigation of the Effect of Body Shape on Sonic-Boom Pressure Distributions.* NASA TN D–3106, 1965.

7. Carlson, Harry W.; and Mack, Robert J.: *A Study of the Sonic-Boom Characteristics of a Blunt Body at a Mach Number of 4.14.* NASA TP–1015, 1977.

8. Mack, Robert J.; and Kuhn, Neil: *Determination of Extrapolation Distance with Measured Pressure Signatures from Two Low-Boom Models.* NASA TM–2004–213264, 2004.

9. Wilcox, Floyd J., Jr.; Elmiligui, Alaa A.; Wayman, Thomas R.; Waithe, Kenrick A.; Howe, Donald C.; and Bangert, Linda S.: *Experimental Sonic Boom Measurements on a Mach 1.6 Cruise Low-Boom Configuration.* NASA TM–2012–217598, 2012.

10. Bobbitt, Percy J.; and Darden, Christine M.: *A Wedge Shaped Supersonic Flow Field Probe.* NASA CP–10133, pp. 379–398, 1994.

11. Bobbitt, Percy J.; Maglieri, Domenic J.; Banks, Daniel W.; and Fuchs, Aaron W.: Wedge and Conical Probes for the Instantaneous Measurement of Free-Stream Flow Quantities at Supersonic Speeds. AIAA Paper 2011–3501, 2011.

12. Wilcox, Floyd J., Jr. and; Elmiligui, Alaa A.: *Experimental Measurements of Sonic Boom Signatures Using a Continuous Data Acquisition Technique.* NASA TP–2013–218035, 2013.

13. Jackson, Charlie M., Jr.; Corlett, William A.; and Monta, William J.: *Description and Calibration of the Langley Unitary Plan Wind Tunnel.* NASA TP–1905, 1981.

14. Mack, Robert J.; and Kuhn, Neil S.: *Determination of Extrapolation Distance With Pressure Signatures Measured at Two to Twenty Span Lengths From Two Low-Boom Models.* NASA TM–2006–214524, 2006.

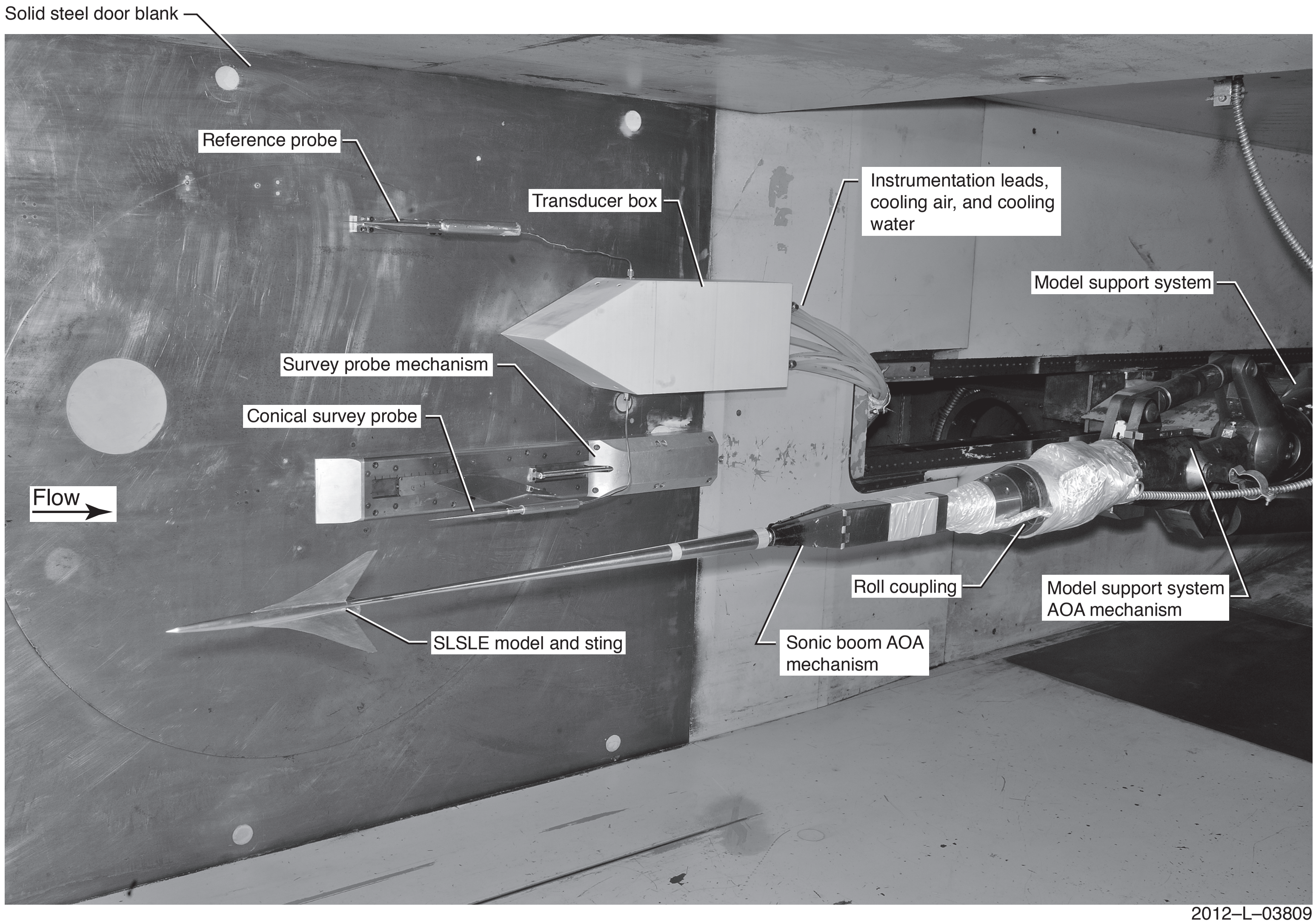

(a) Model mounted in wind tunnel.

Figure 1. General experimental test setup for the conical survey probe.

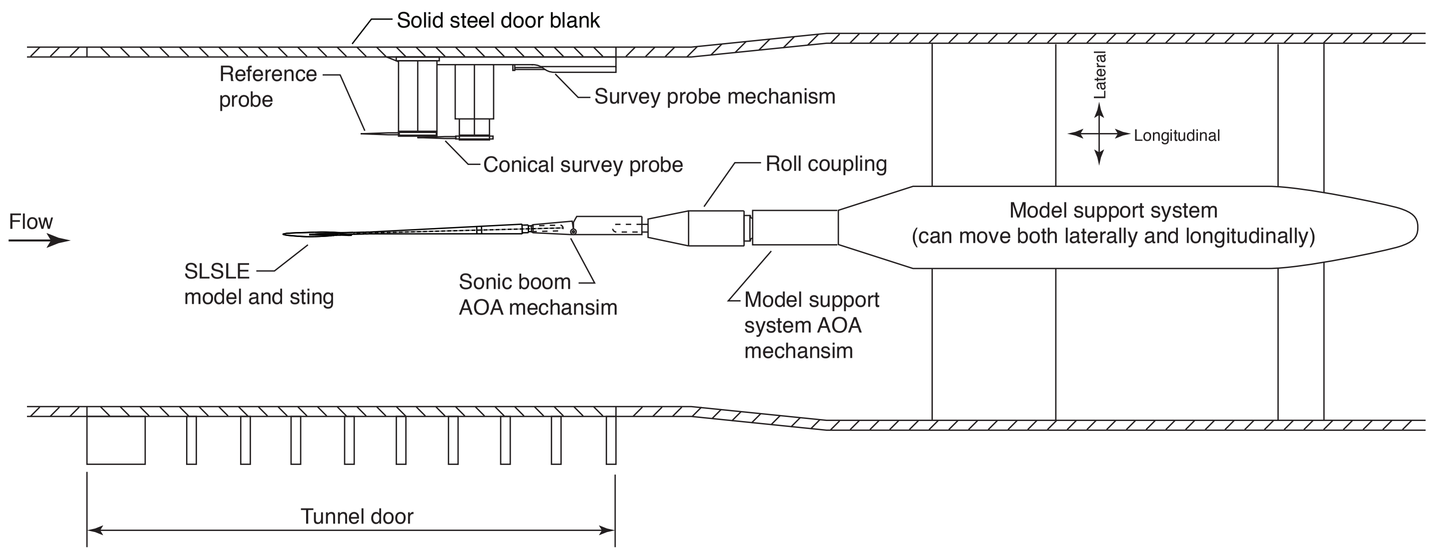

(b) Top view (transducer box removed for clarity).

Figure 1. Concluded.

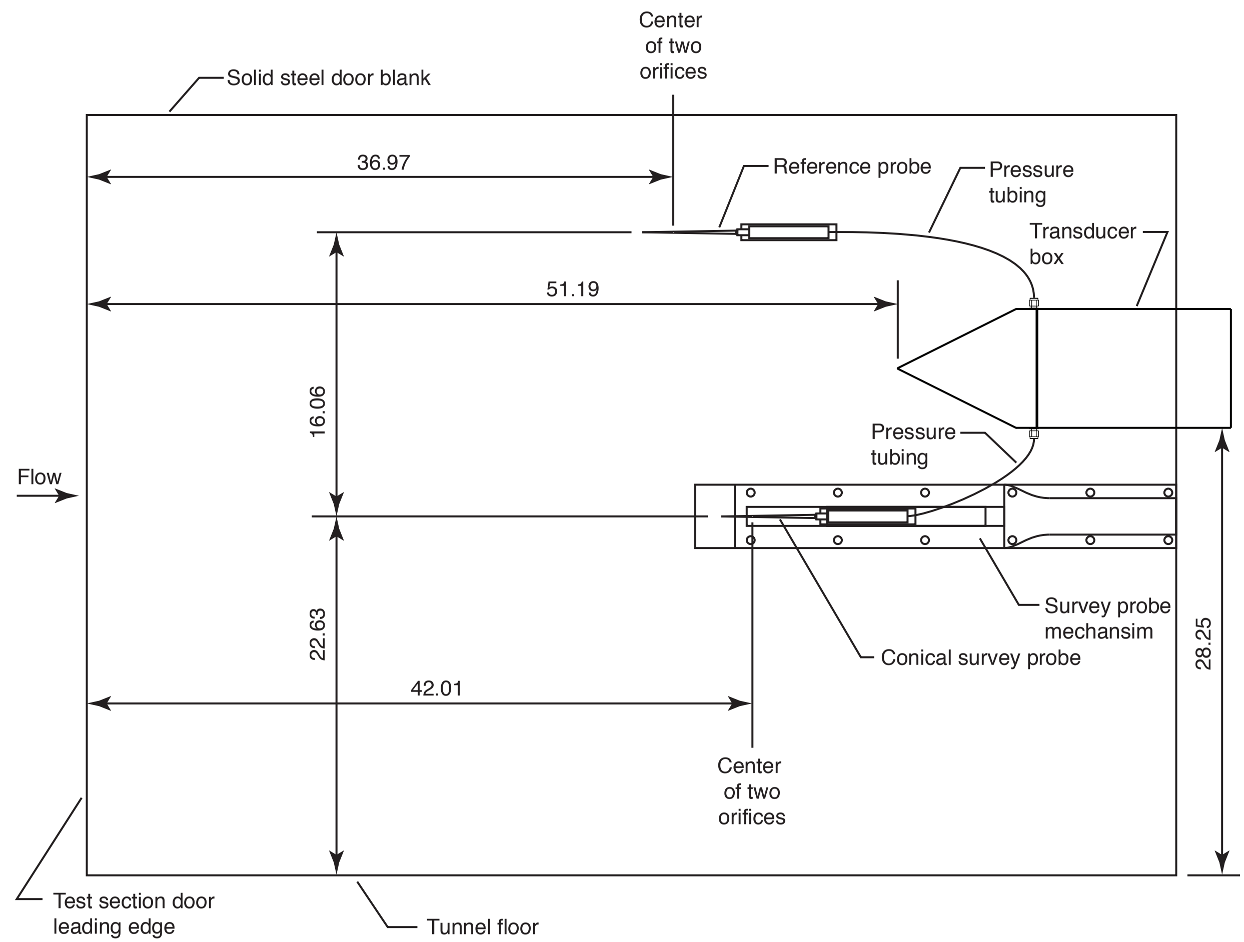

(a) Side view.

Figure 2. Details of the experimental setup for the conical survey probe. All dimensions are in inches.

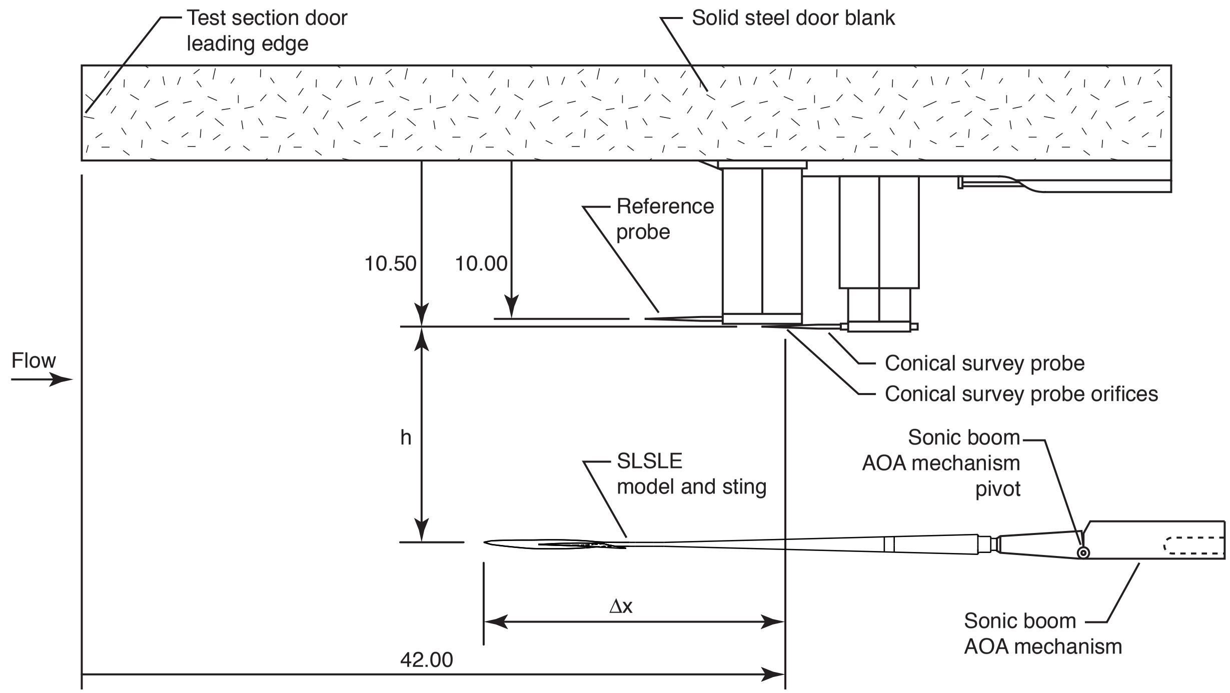

(b) Top view (transducer box removed for clarity).

Figure 2. Concluded.

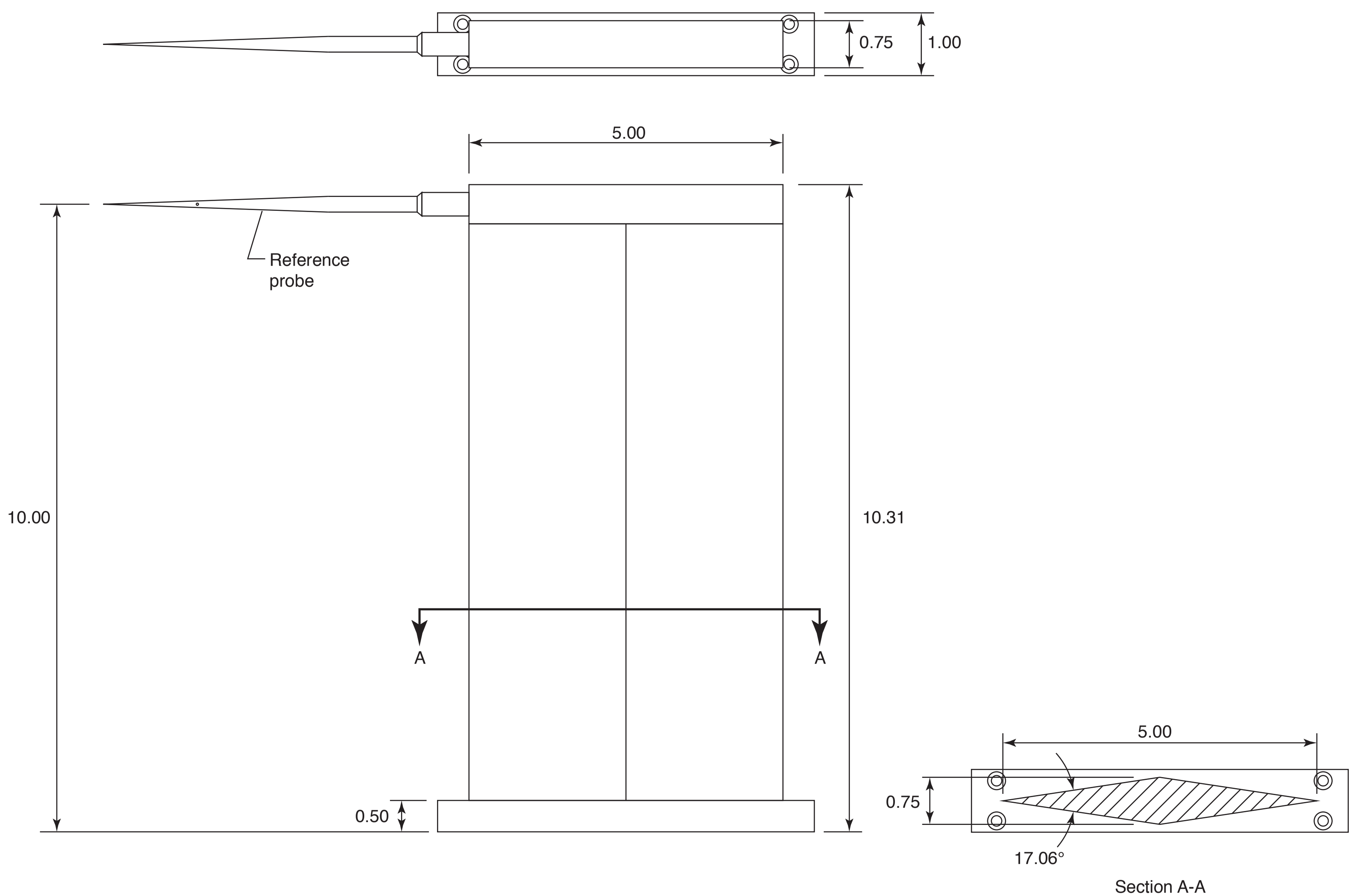

(a) Reference probe holder.

Figure 3. Various hardware sketches. All dimensions are in inches unless otherwise noted.

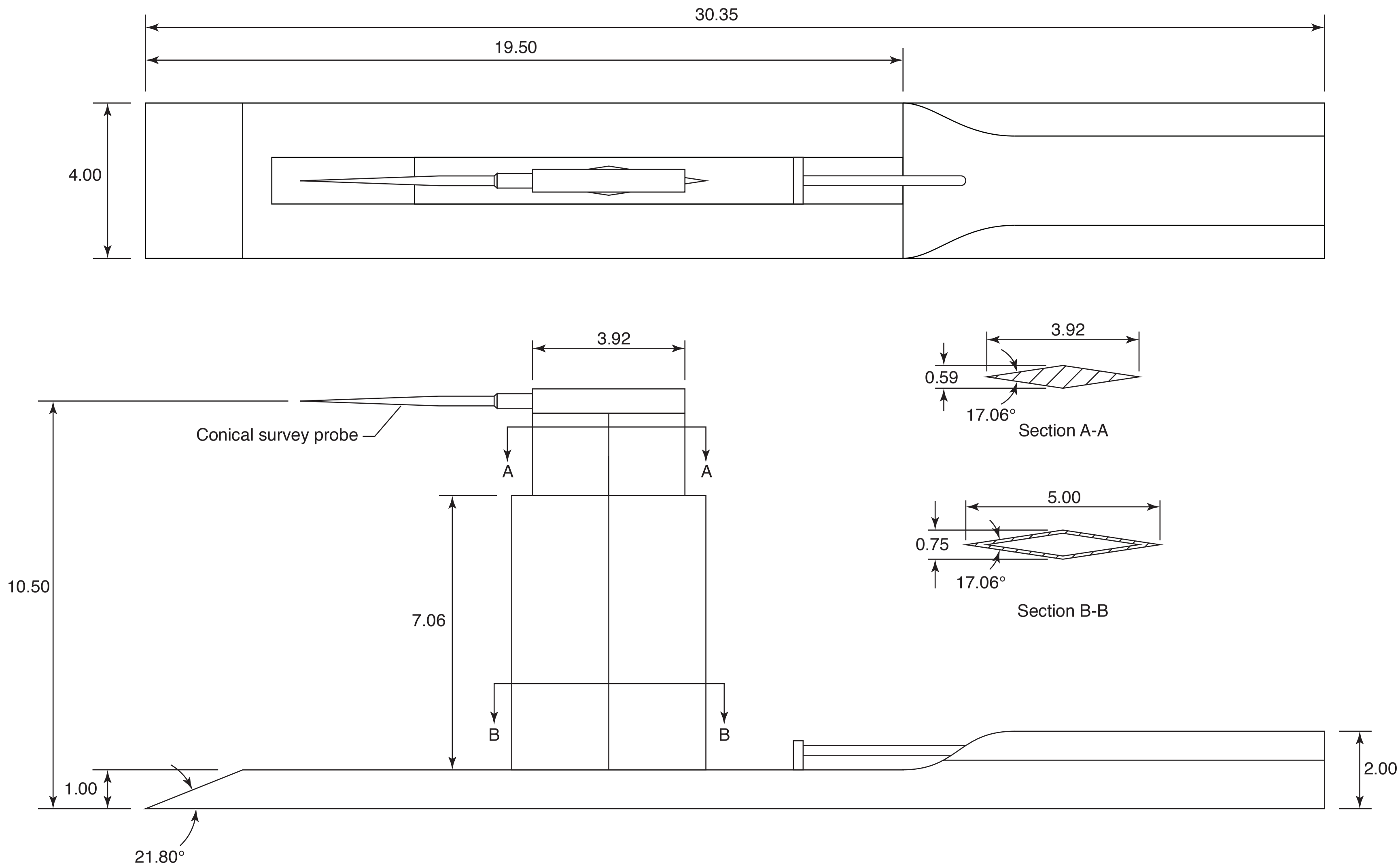

(b) Survey probe mechanism.

Figure 3. Continued.

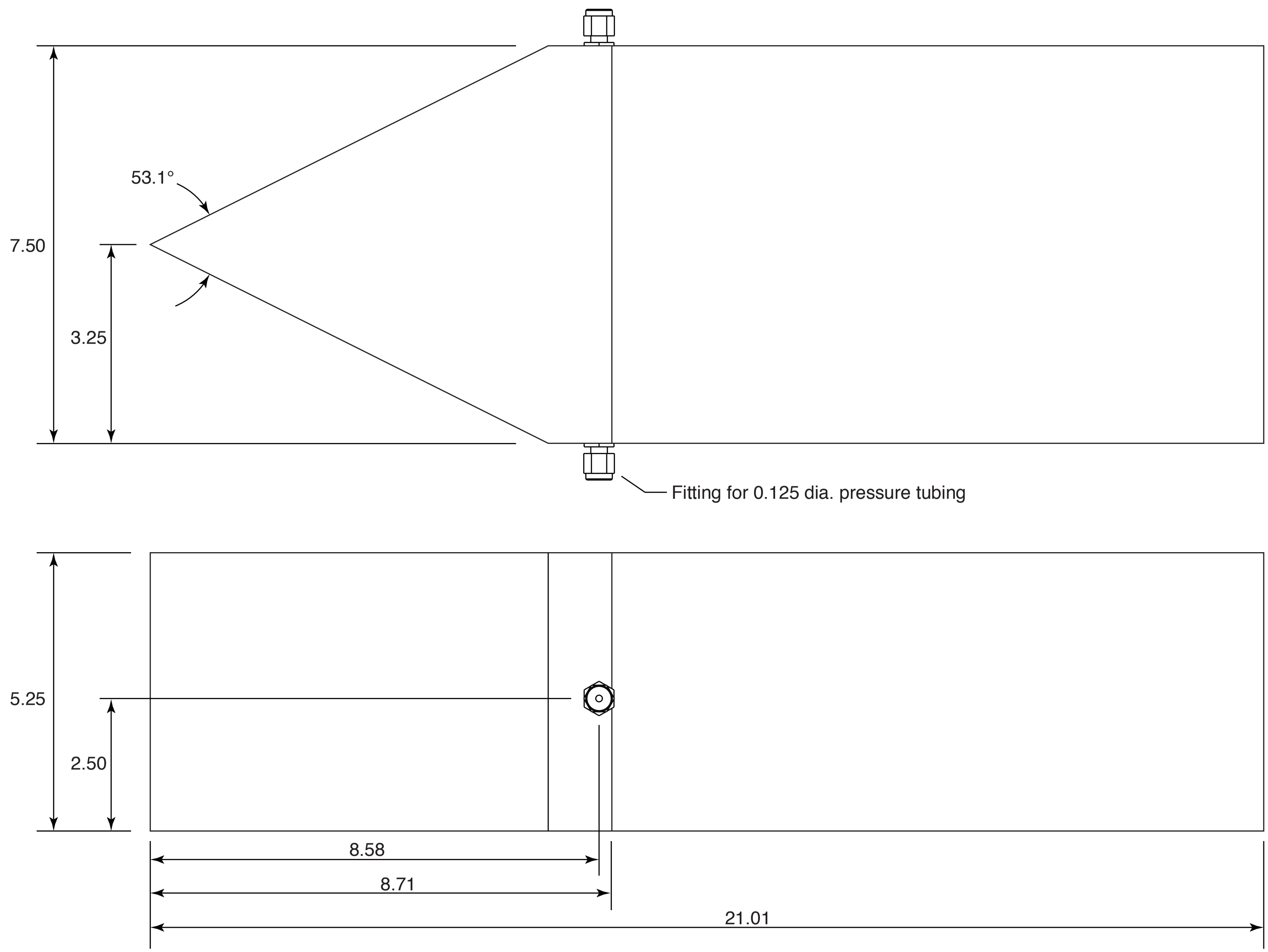

(c) Transducer box.

Figure 3. Concluded.

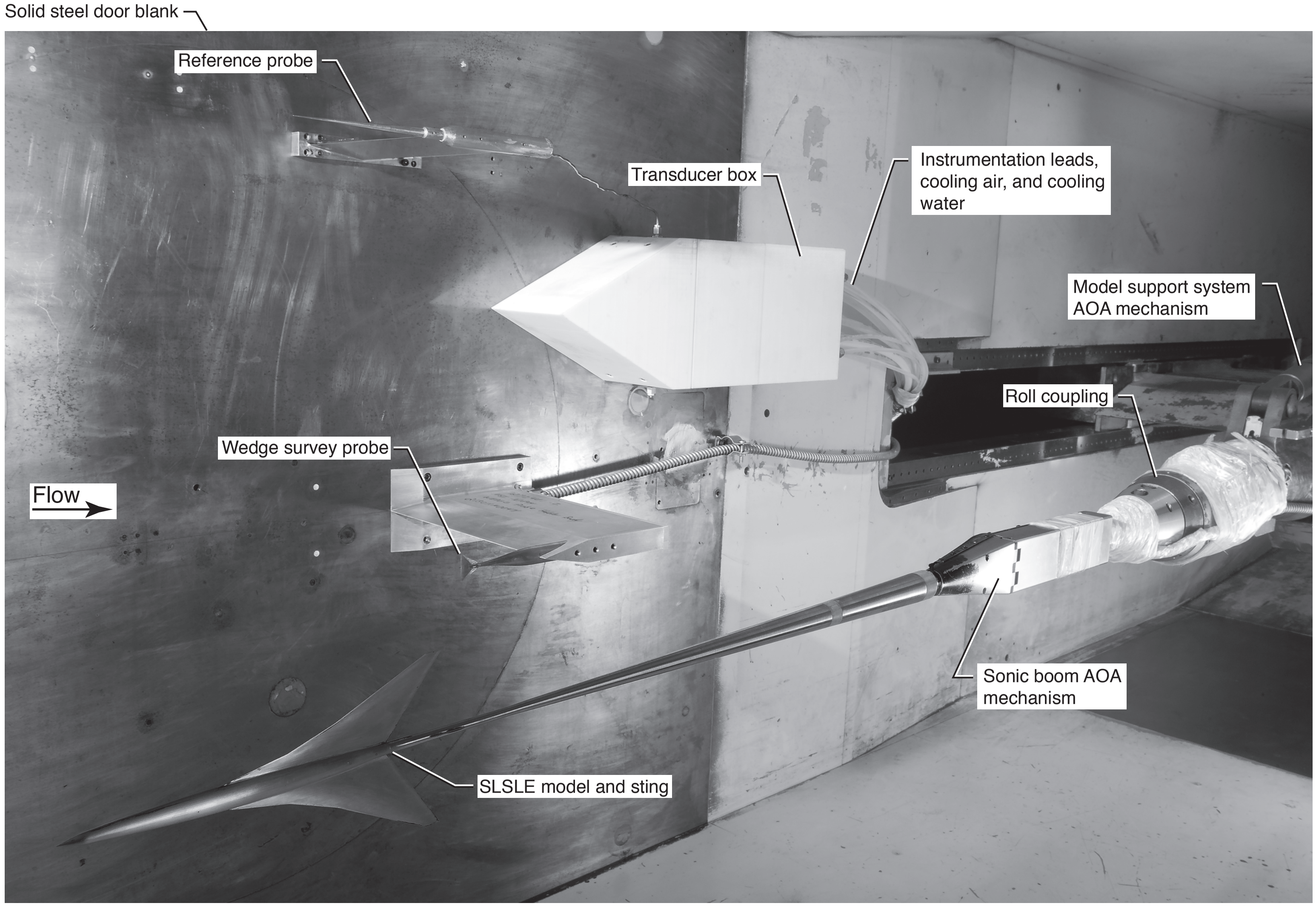

(a) Model mounted in wind tunnel.

Figure 4. General experimental test setup for the wedge survey probe.

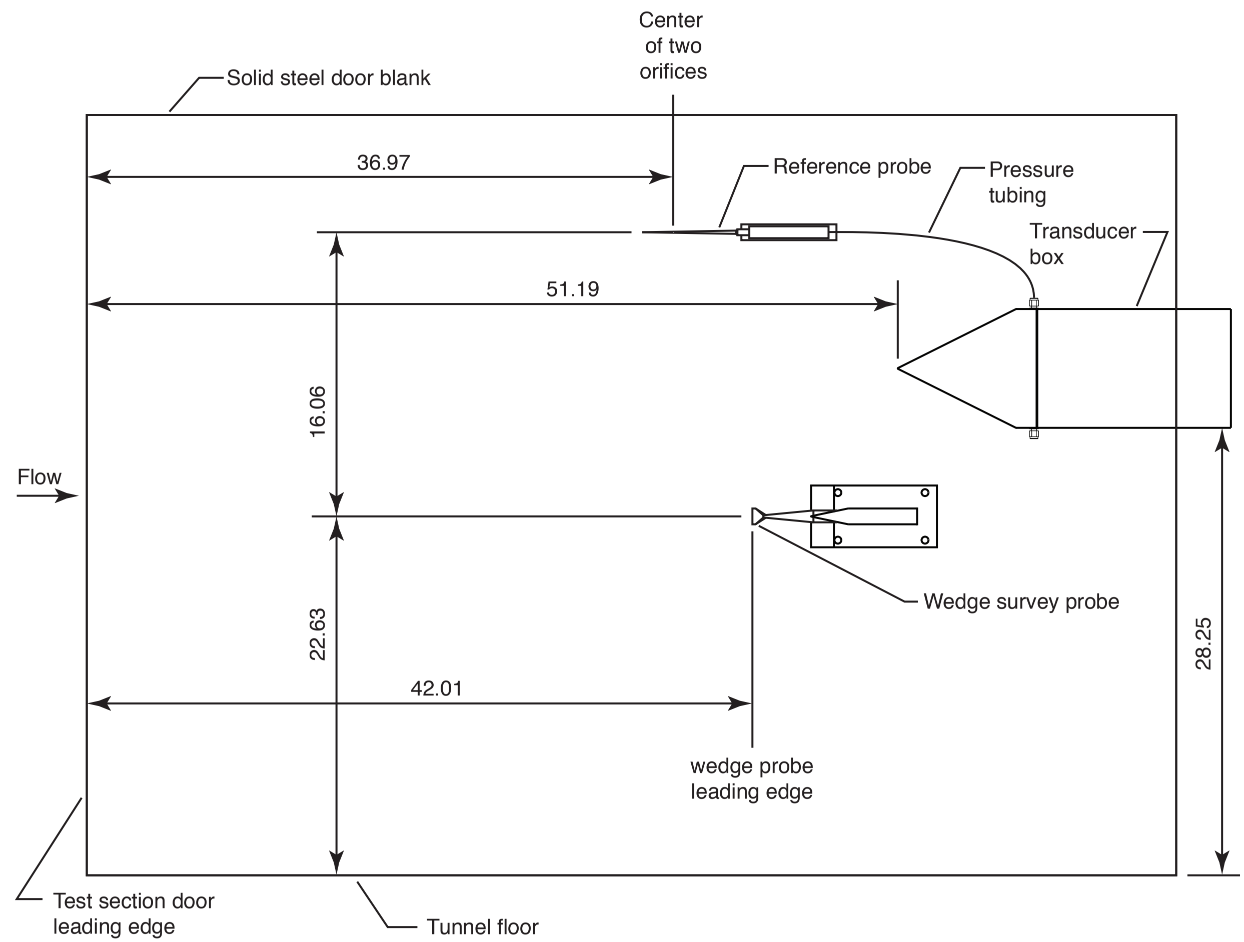

(b) Side view.

Figure 4. Continued.

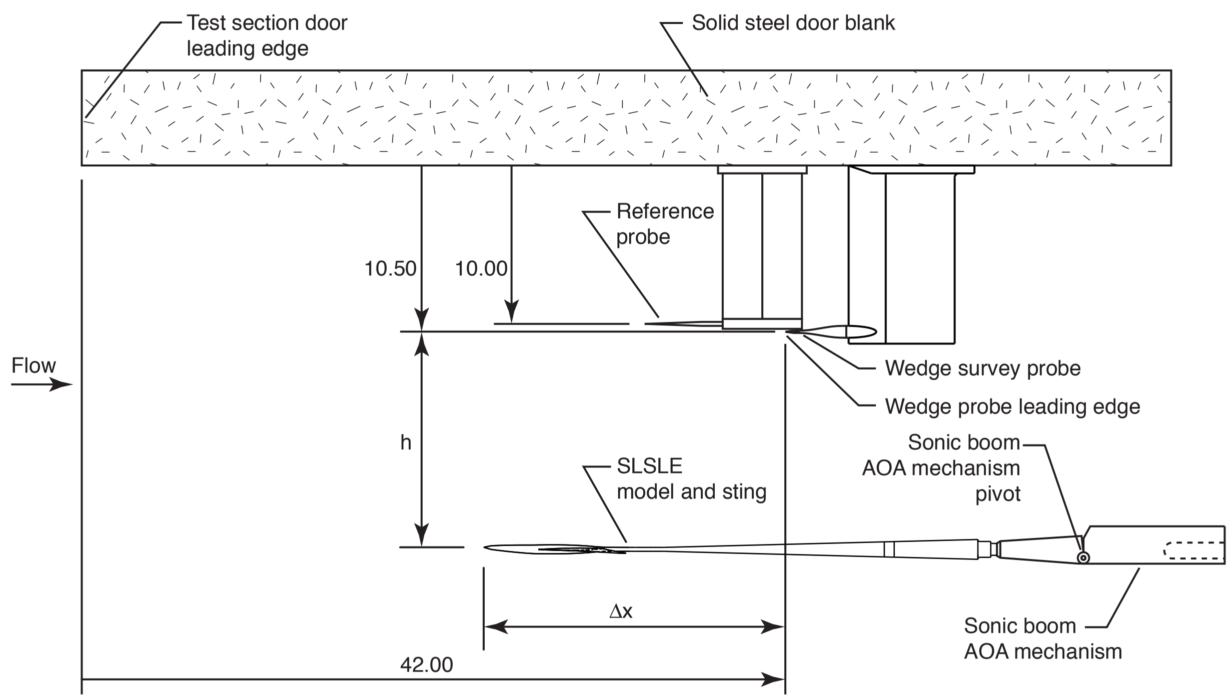

(c) Top view (transducer box removed for clarity).

Figure 4. Concluded.

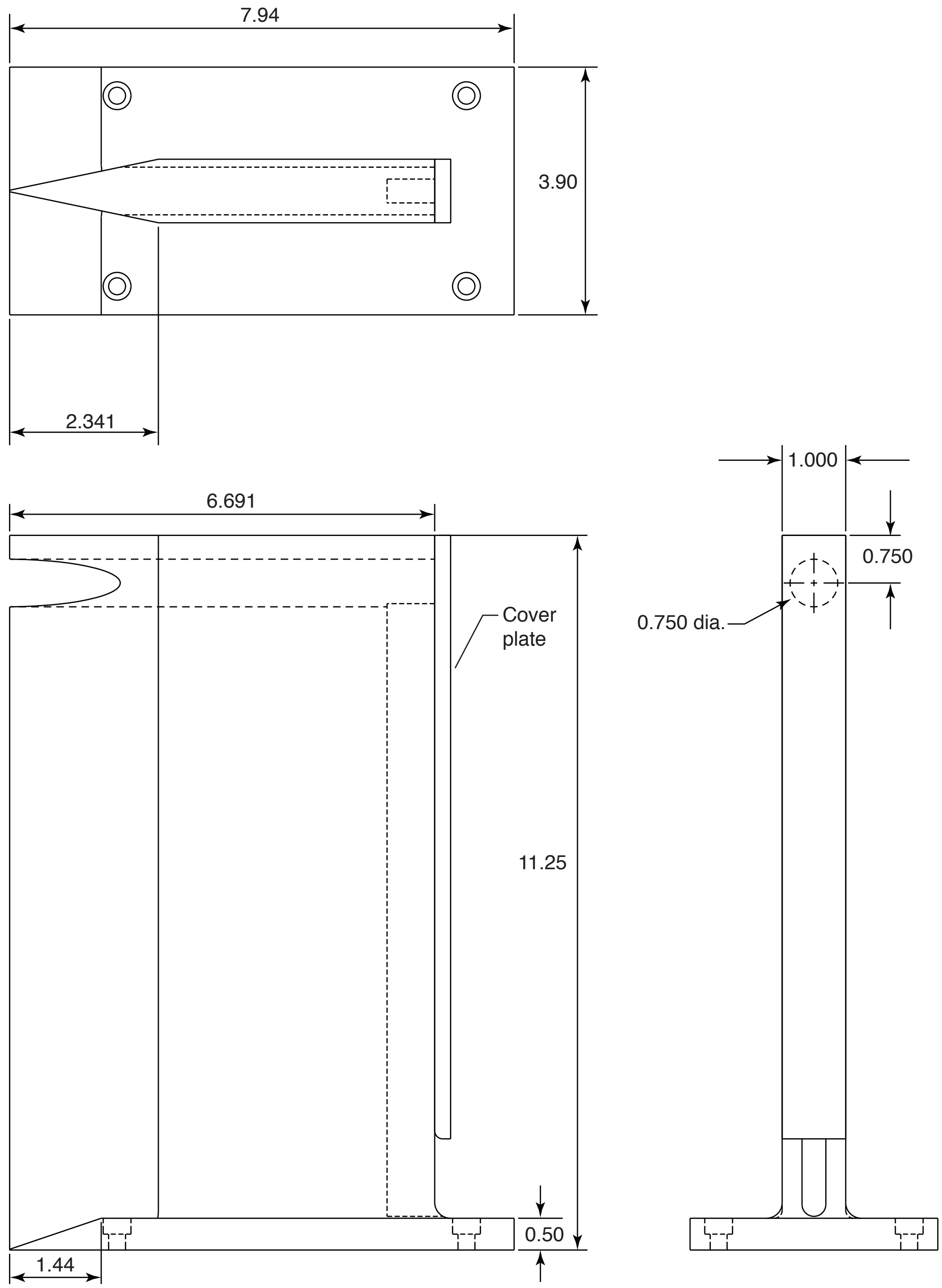

Figure 5. Wedge probe holder. Dimensions are in inches.

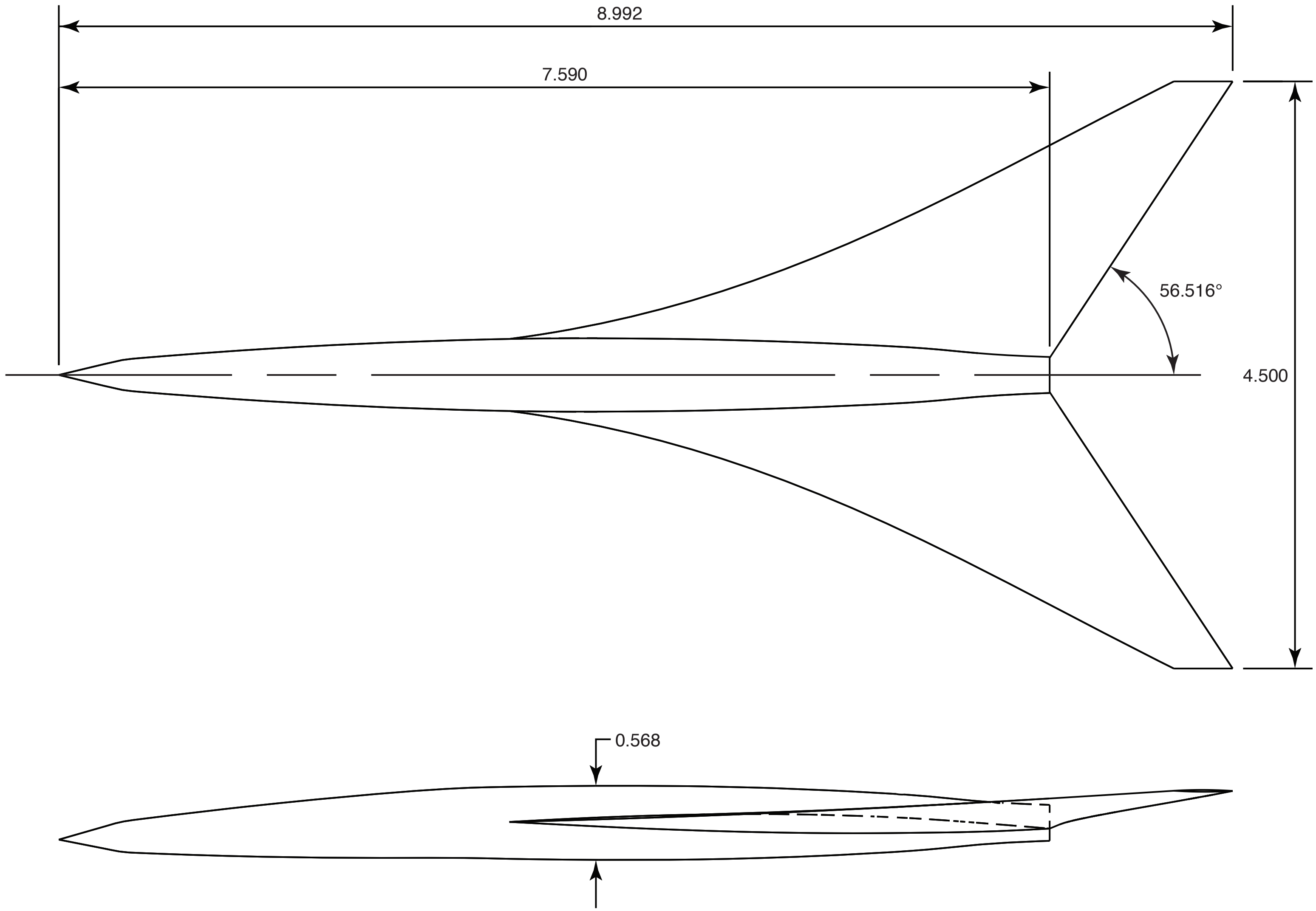

(a) Overall dimensions.

Figure 6. Straight-line segmented leading edge model description. All dimensions are in inches unless otherwise noted.

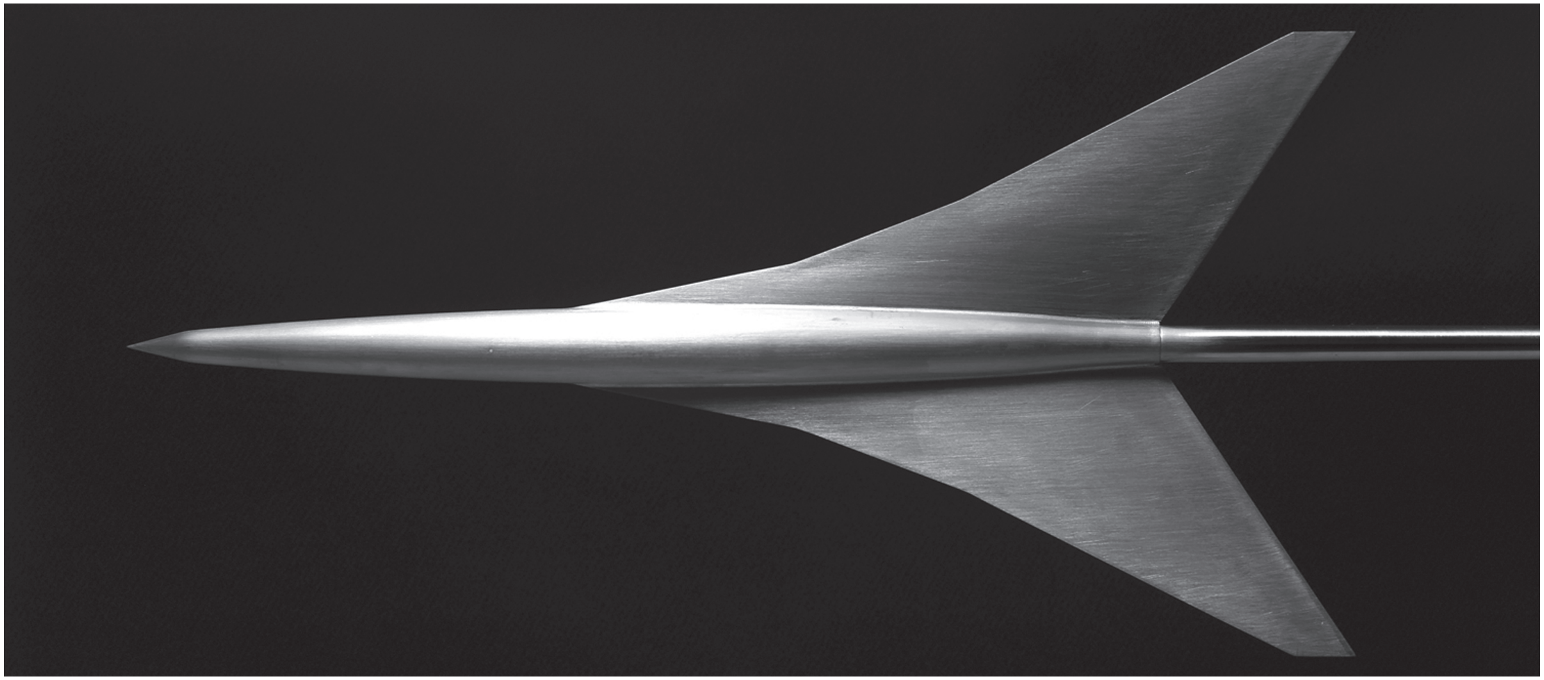

L–2003–01611

(b) Top view.

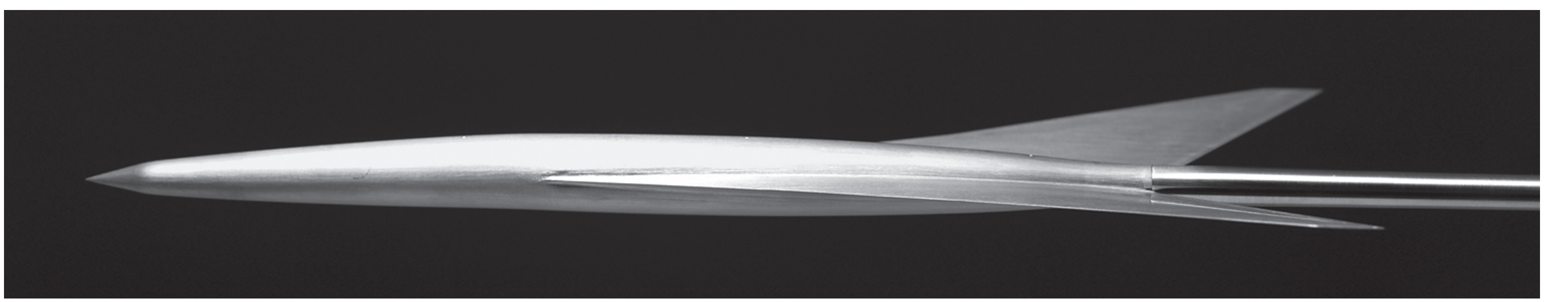

L–2003–01612

(c) Side view.

Figure 6. Concluded.

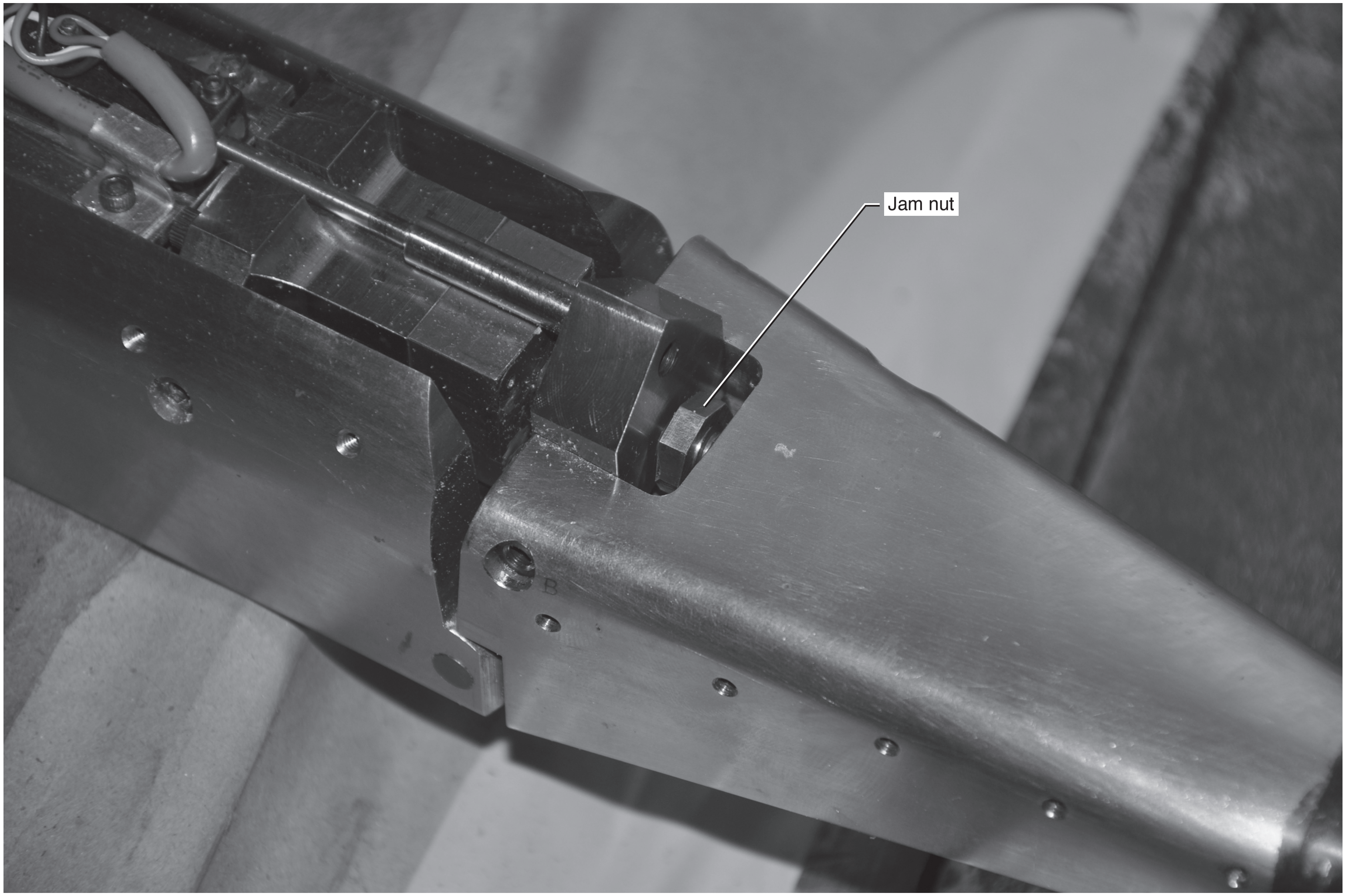

Figure 7. Jam nut used to lock the position of the sonic boom AOA mechanism.

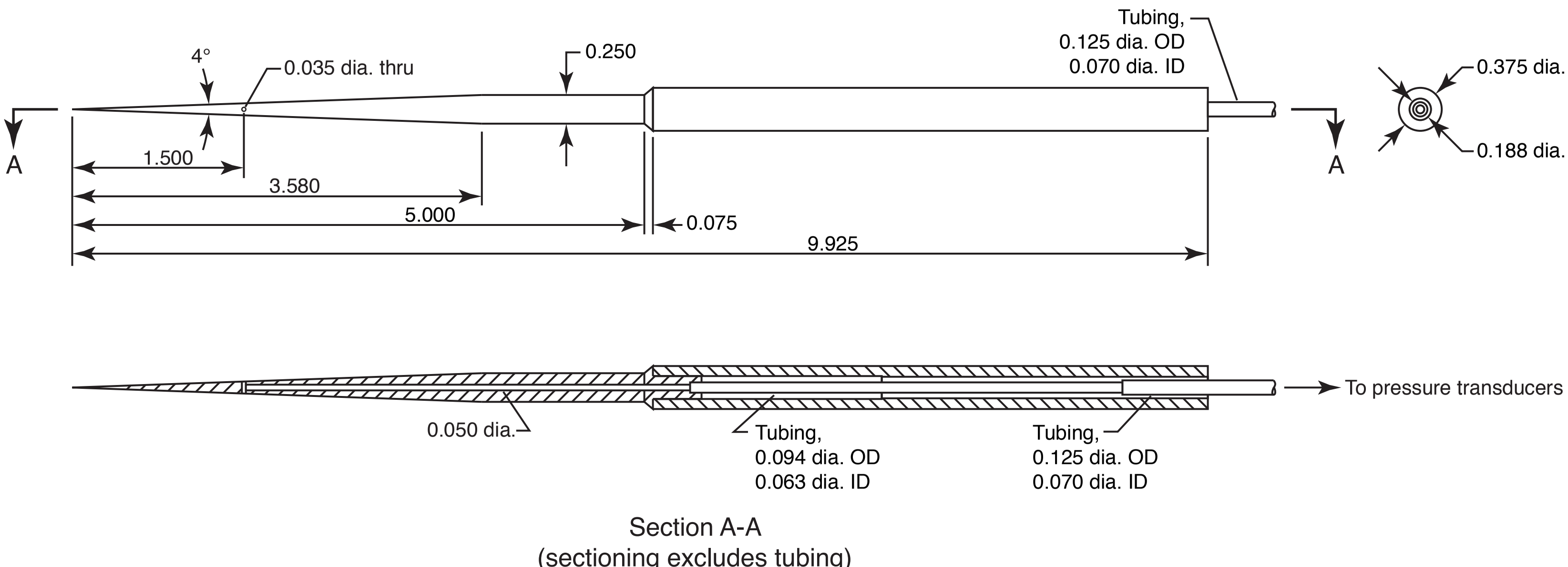

Tubing lengths (approximate)

Probe	0.094 dia. OD	0.0125 dia. OD
Reference	15	7
Survey	3	19

Figure 8. Conical reference and survey probe drawing. All dimensions are in inches unless otherwise noted.

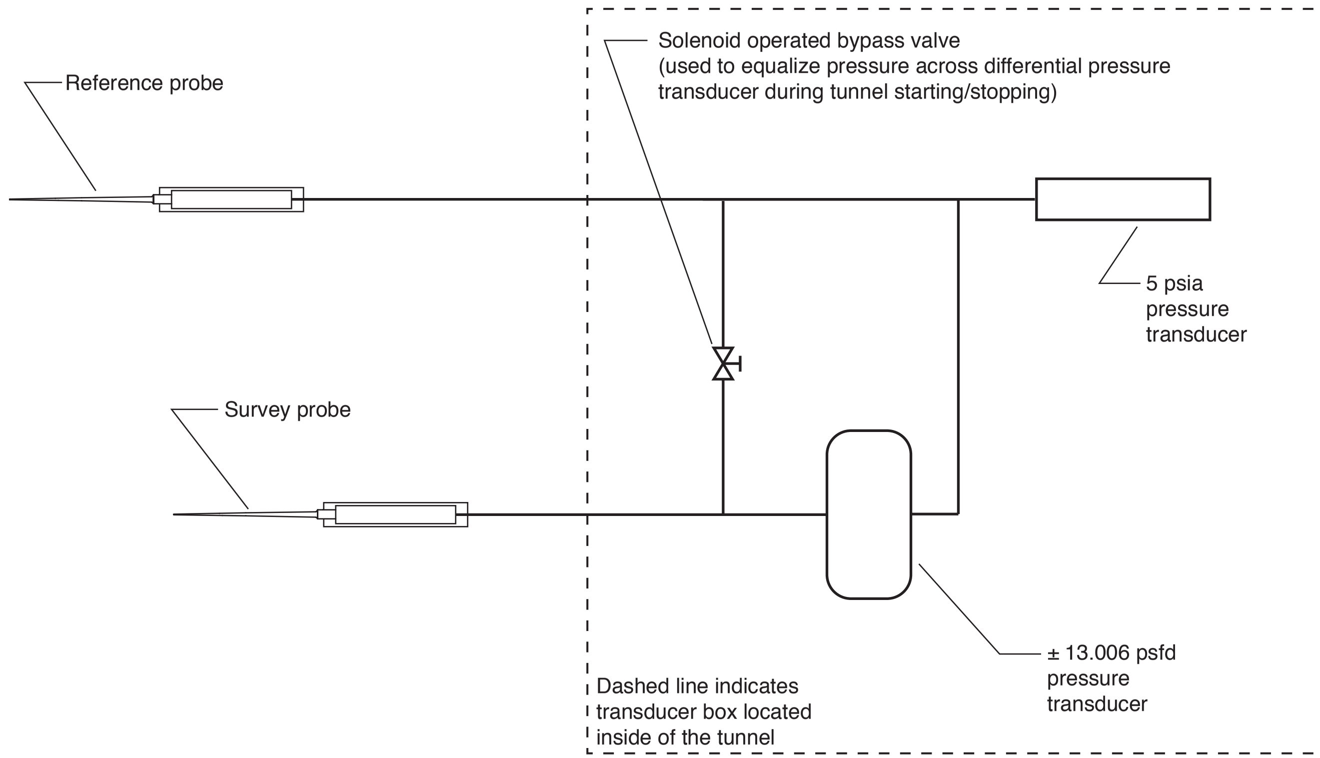

Figure 9. Conical reference and survey probe pressure hookup.

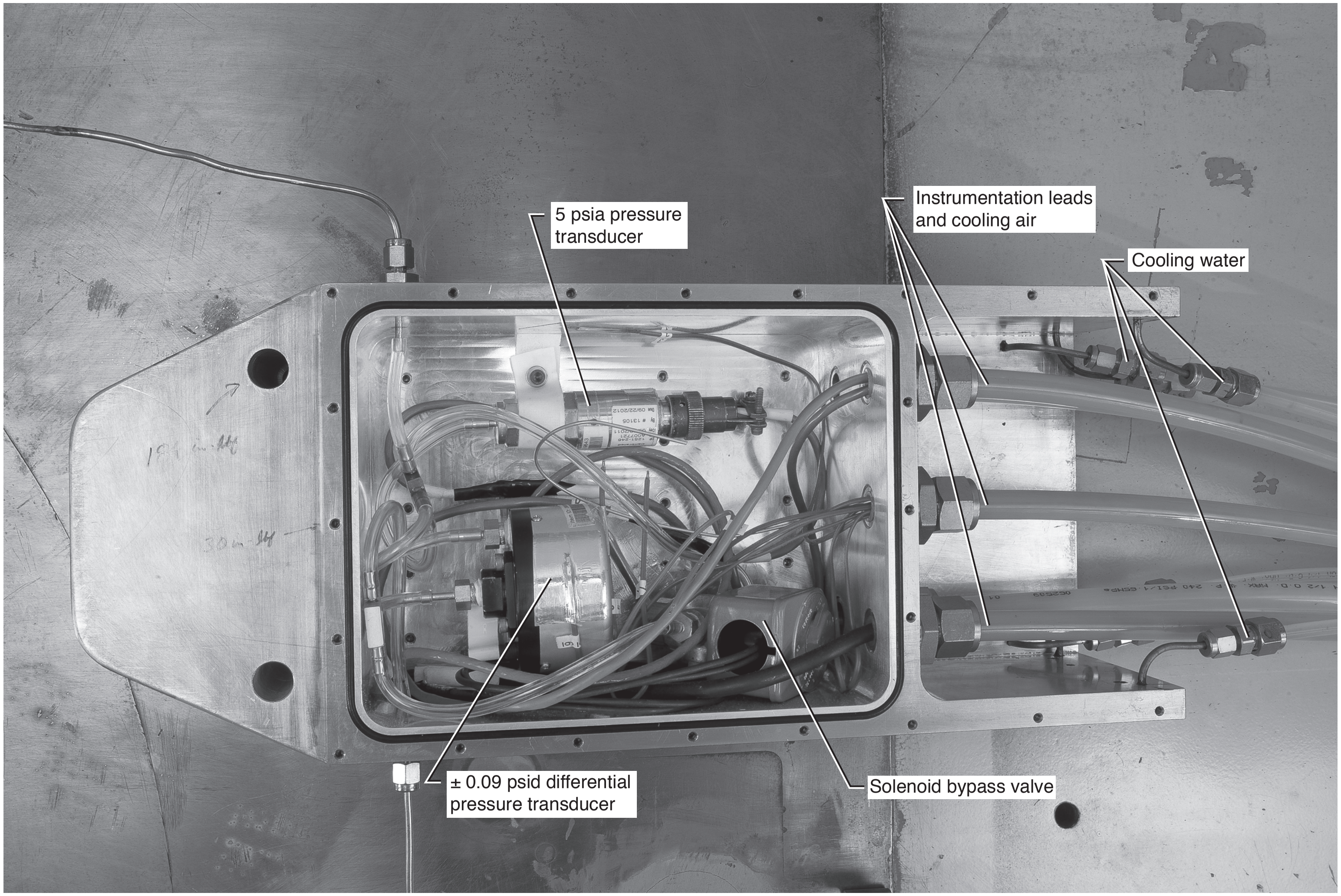

2012–L–03808

Figure 10. Transducer box (insulating plastic cover removed).

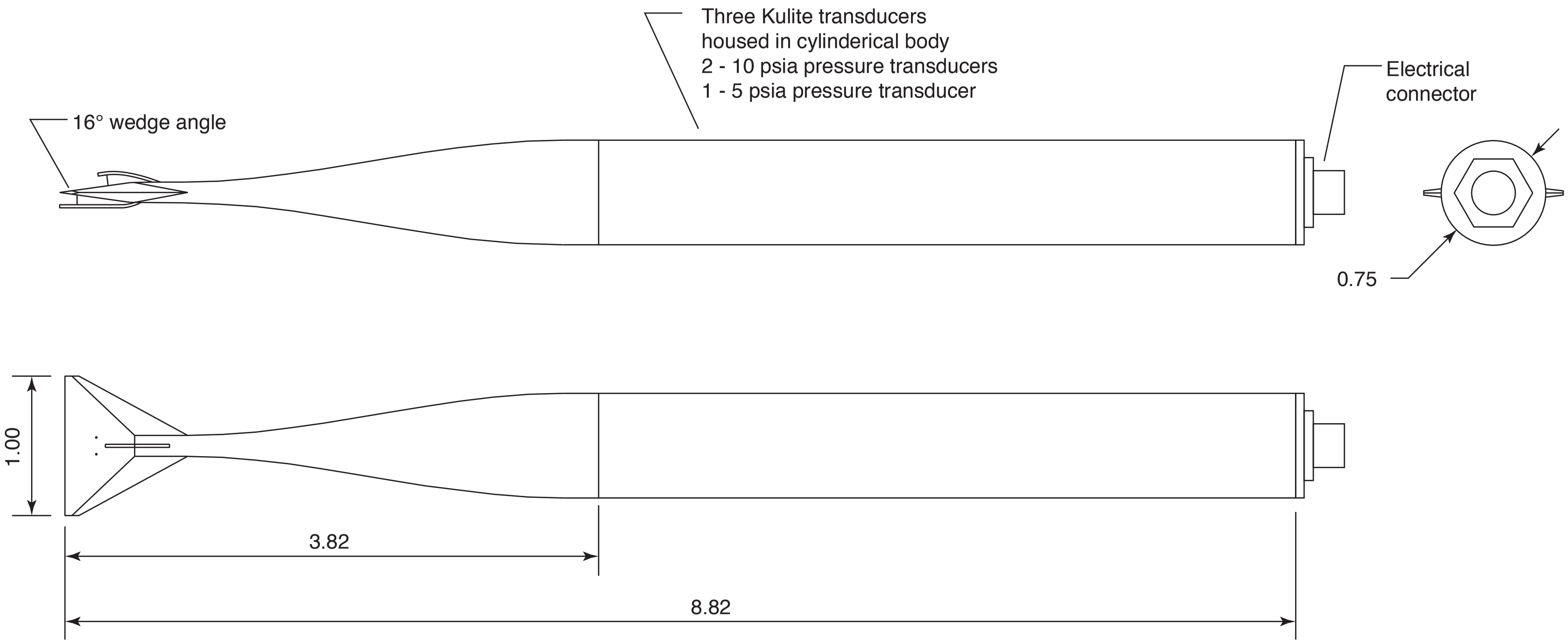

(a) Overall dimensions.

Figure 11. Wedge probe details. All dimensions in inches unless otherwise noted.

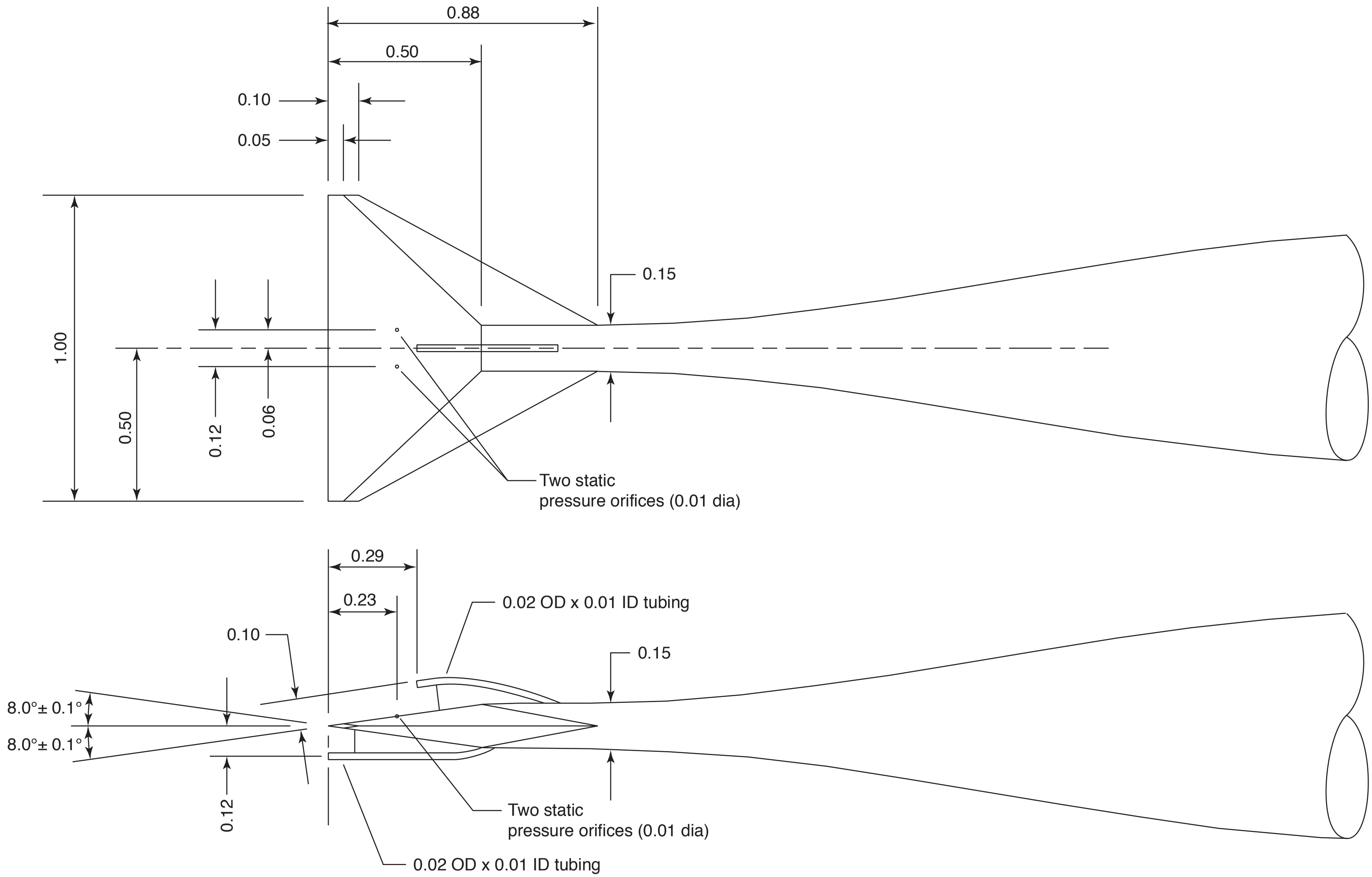

(b) Wedge details.

Figure 11. Continued.

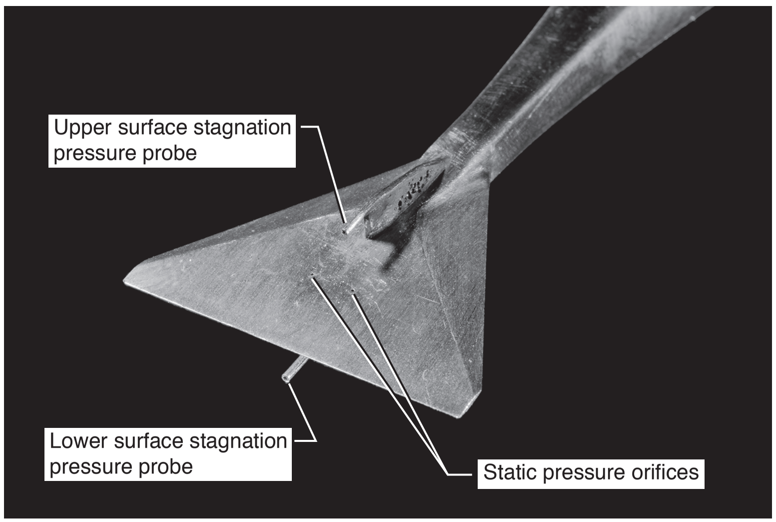

(c) Upper surface.

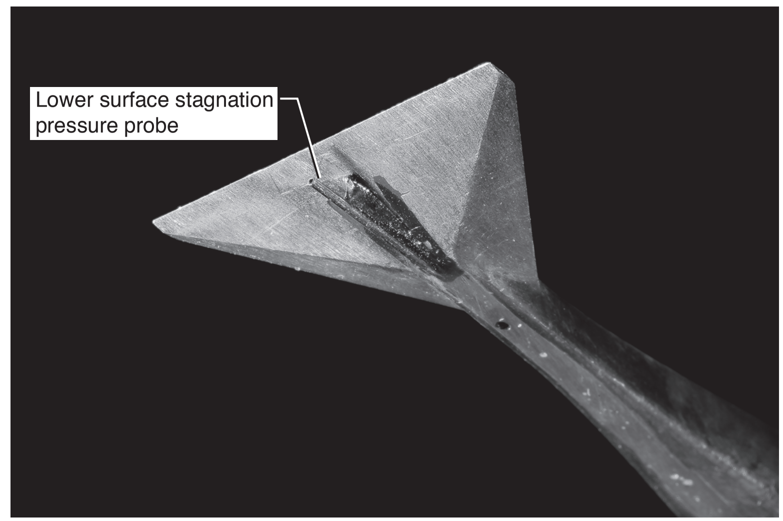

(d) Lower surface.

Figure 11. Concluded.

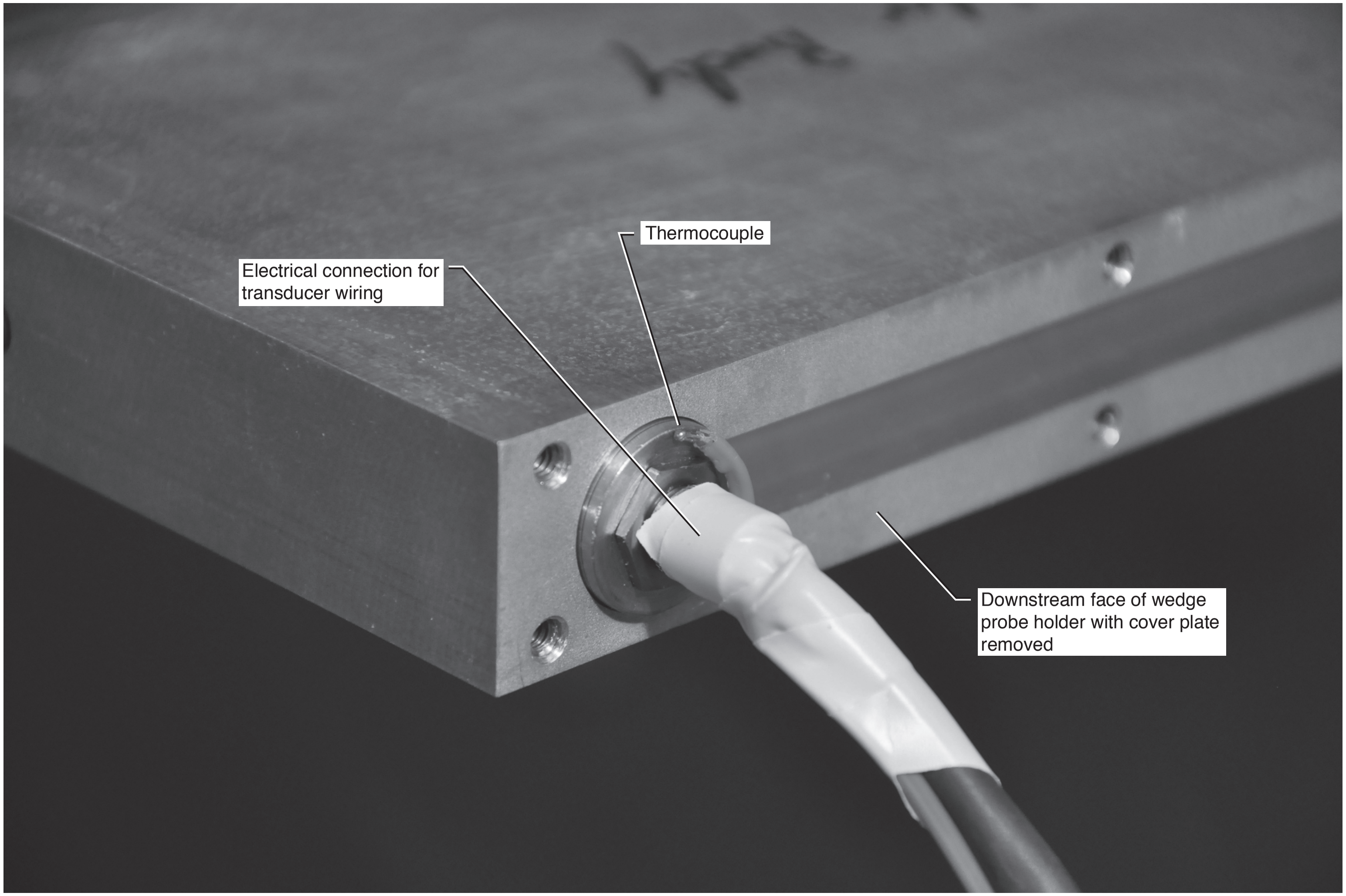

Figure 12. Thermocouple attached to aft end of wedge probe.

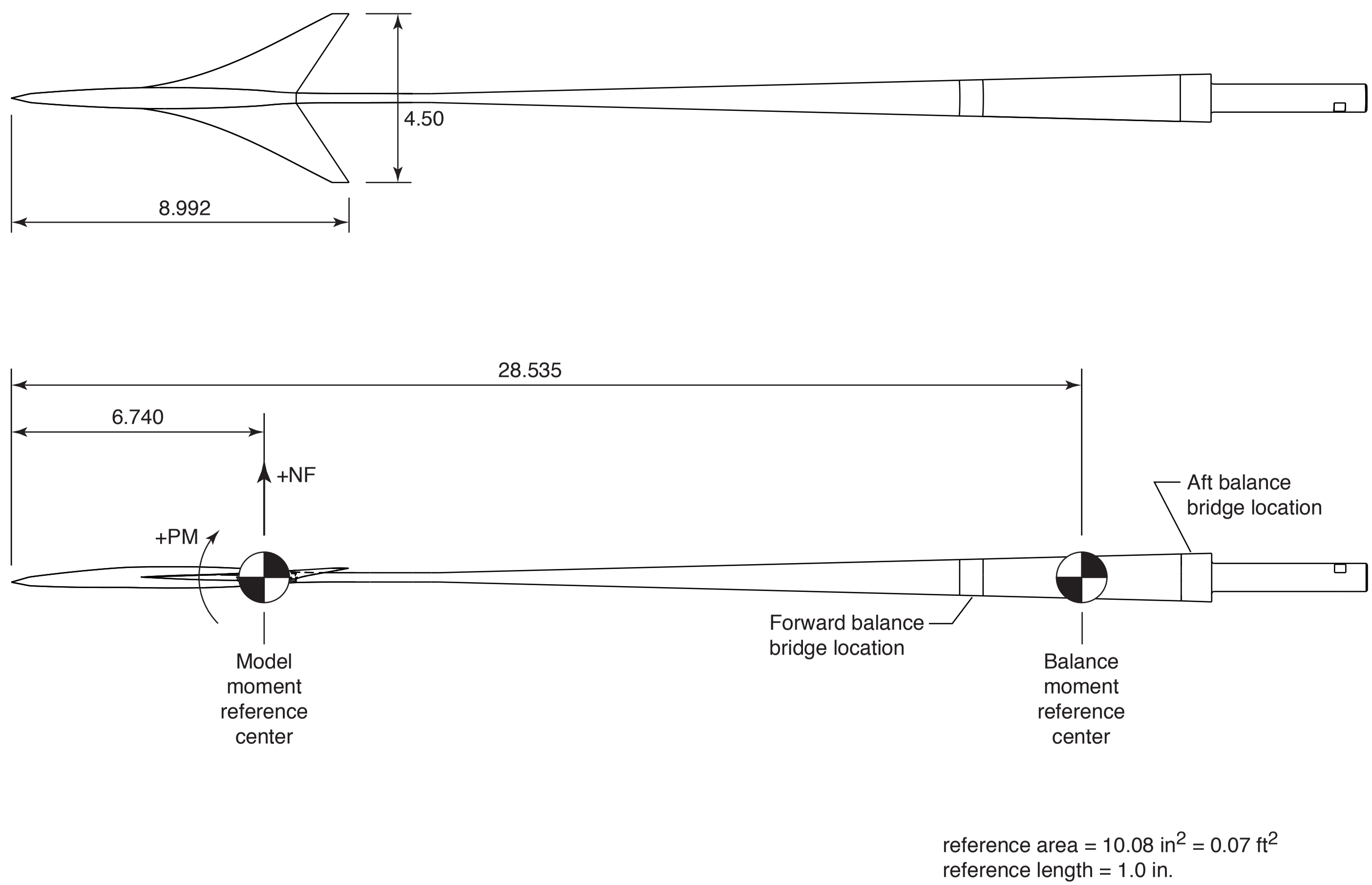

Figure 13. Moment reference center locations. All dimensions are in inches.

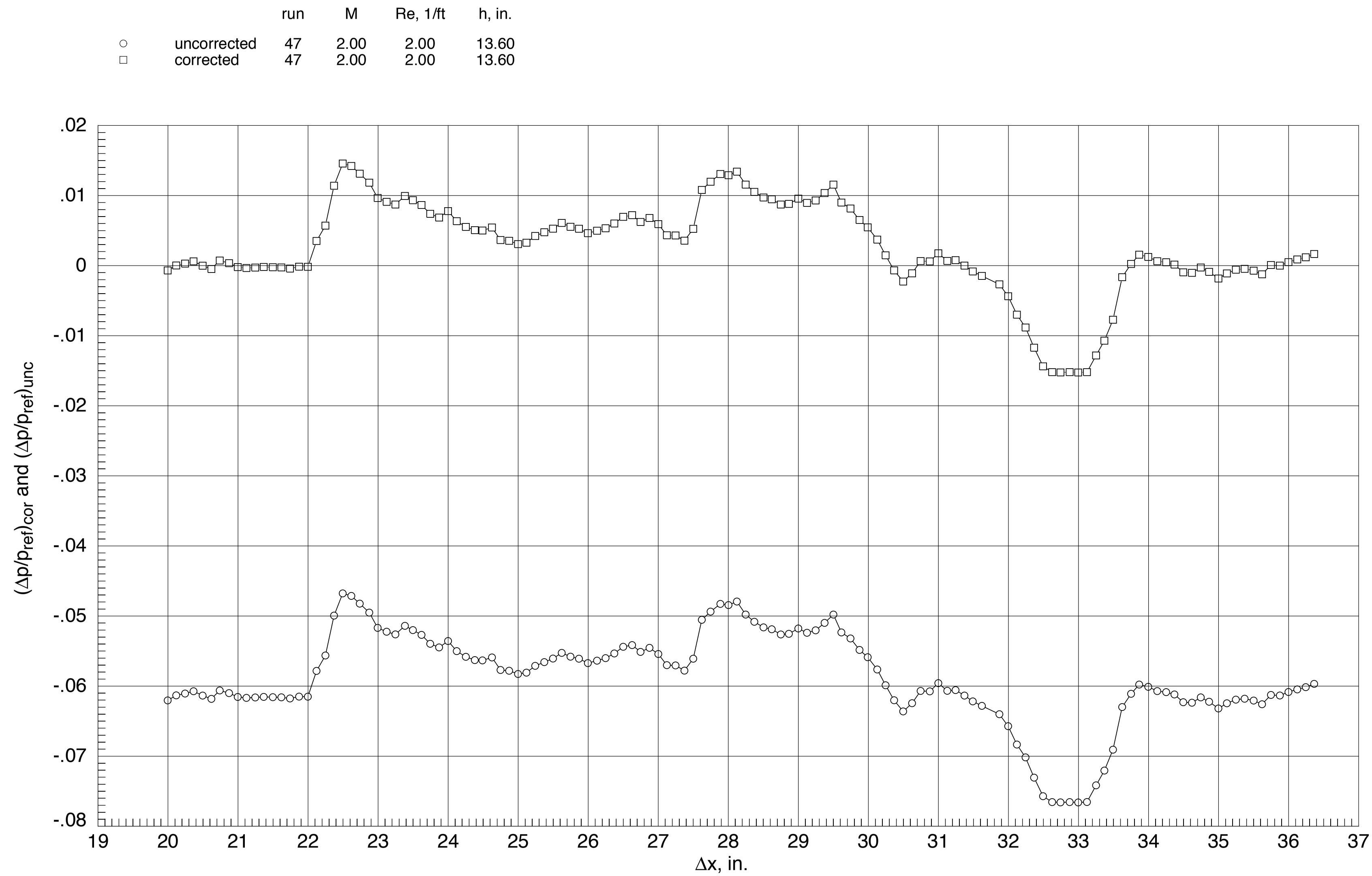

(a) Conical survey probe.

Figure 14. Comparison of uncorrected and corrected sonic boom pressure signatures.

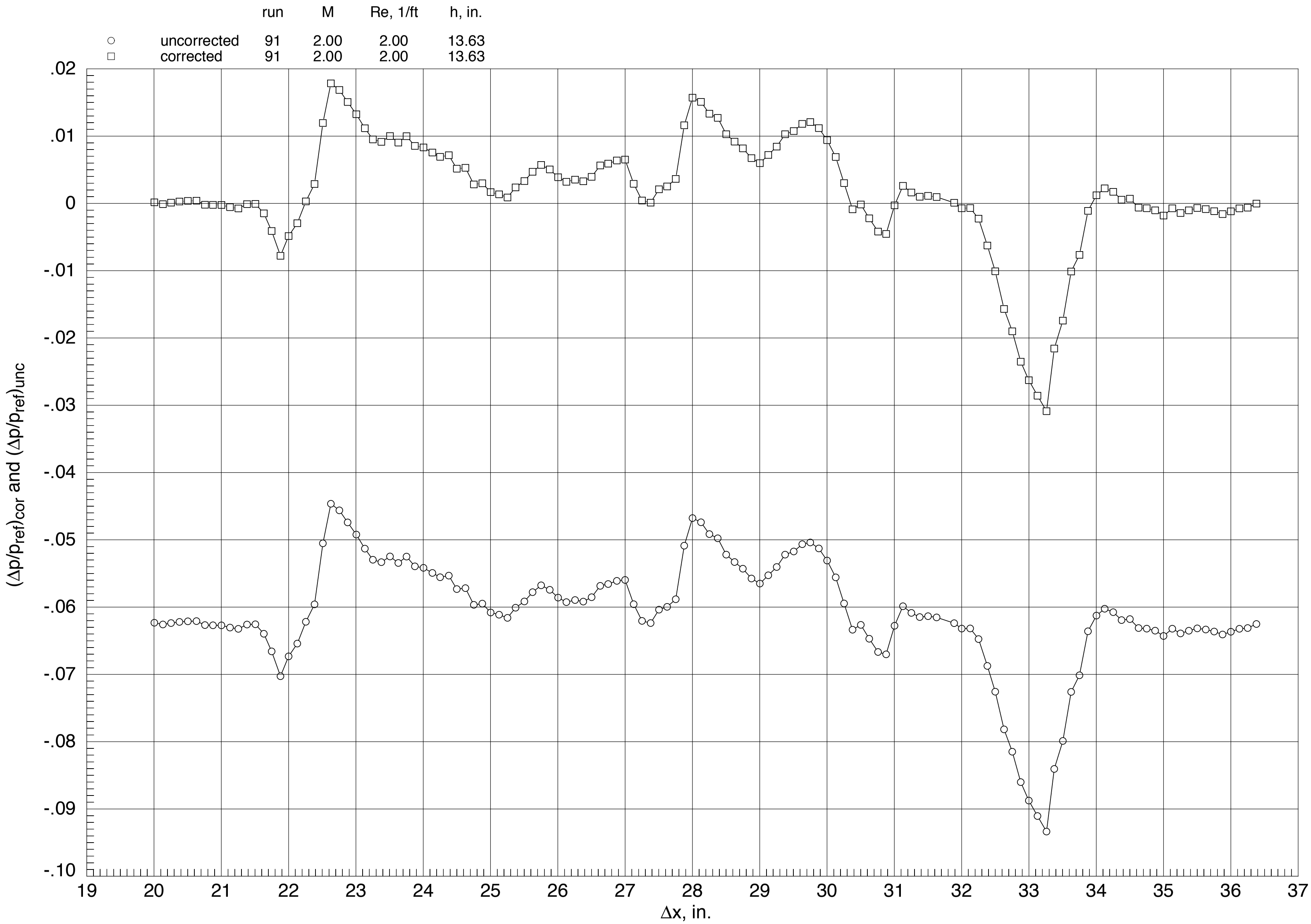

(b) Wedge survey probe.

Figure 14. Concluded.

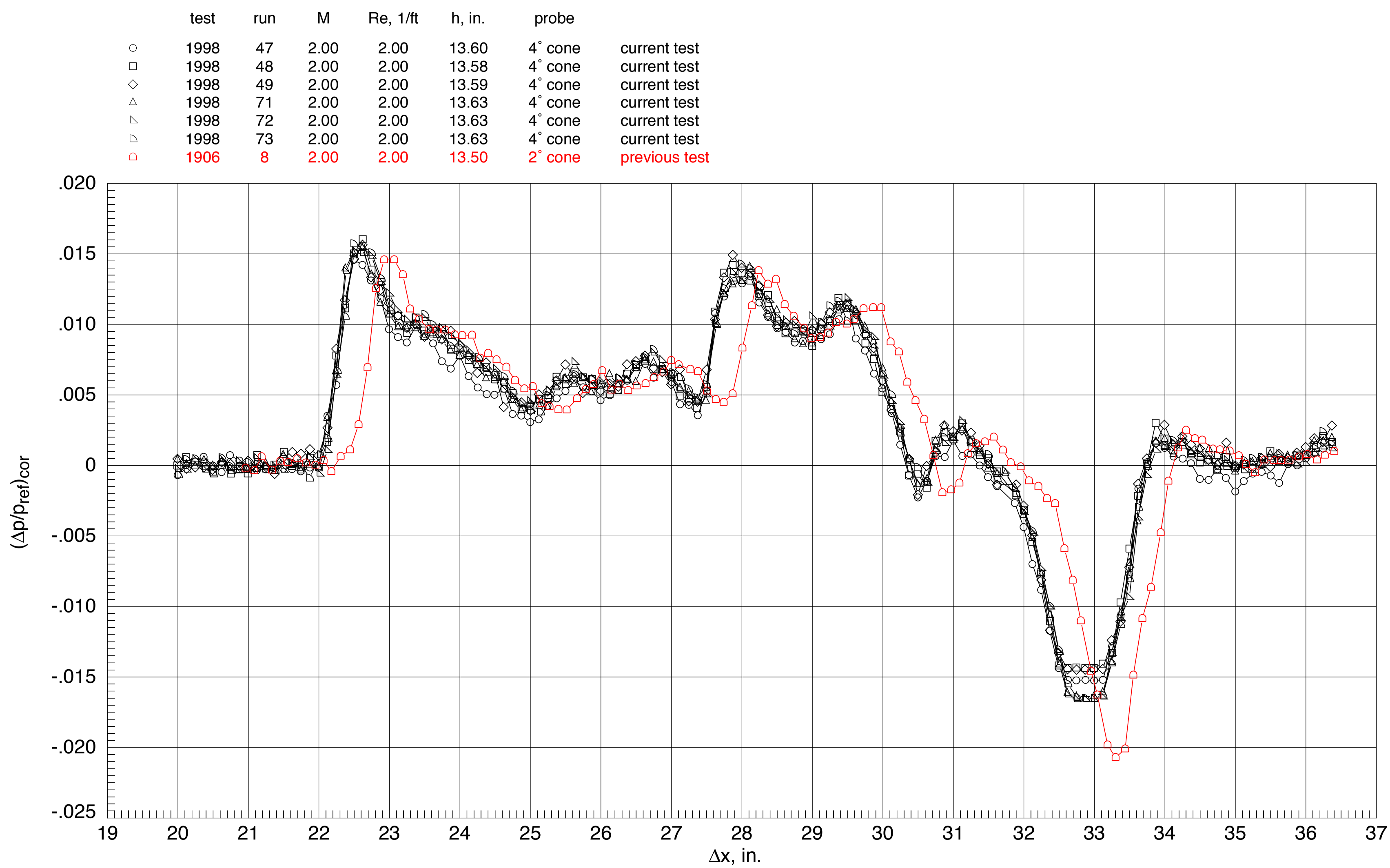

Figure 15. Sonic boom pressure signature comparison between tests.

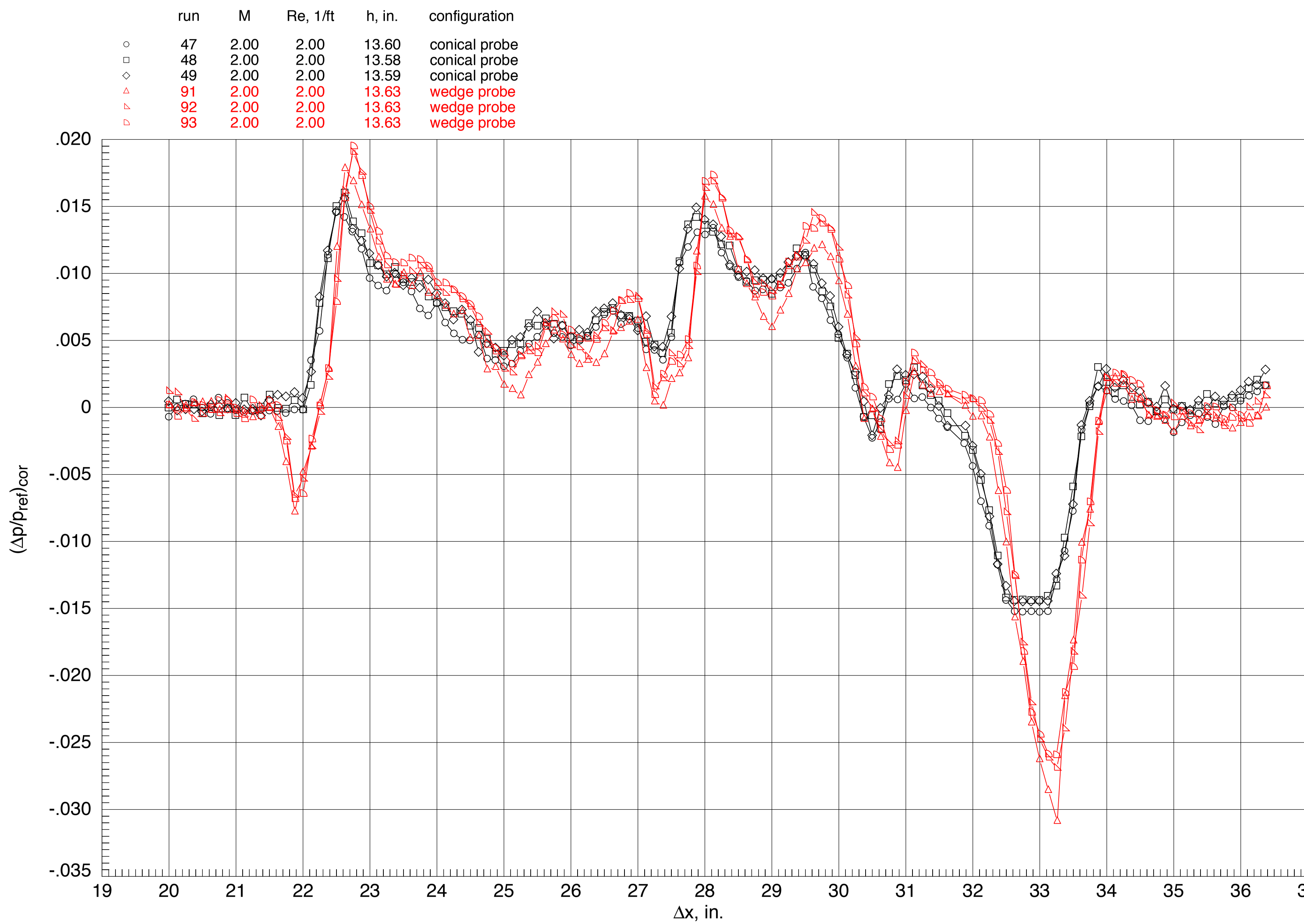

(a) First set of repeats.

Figure 16. Comparison of sonic boom pressure signatures obtained with conical and wedge probes.

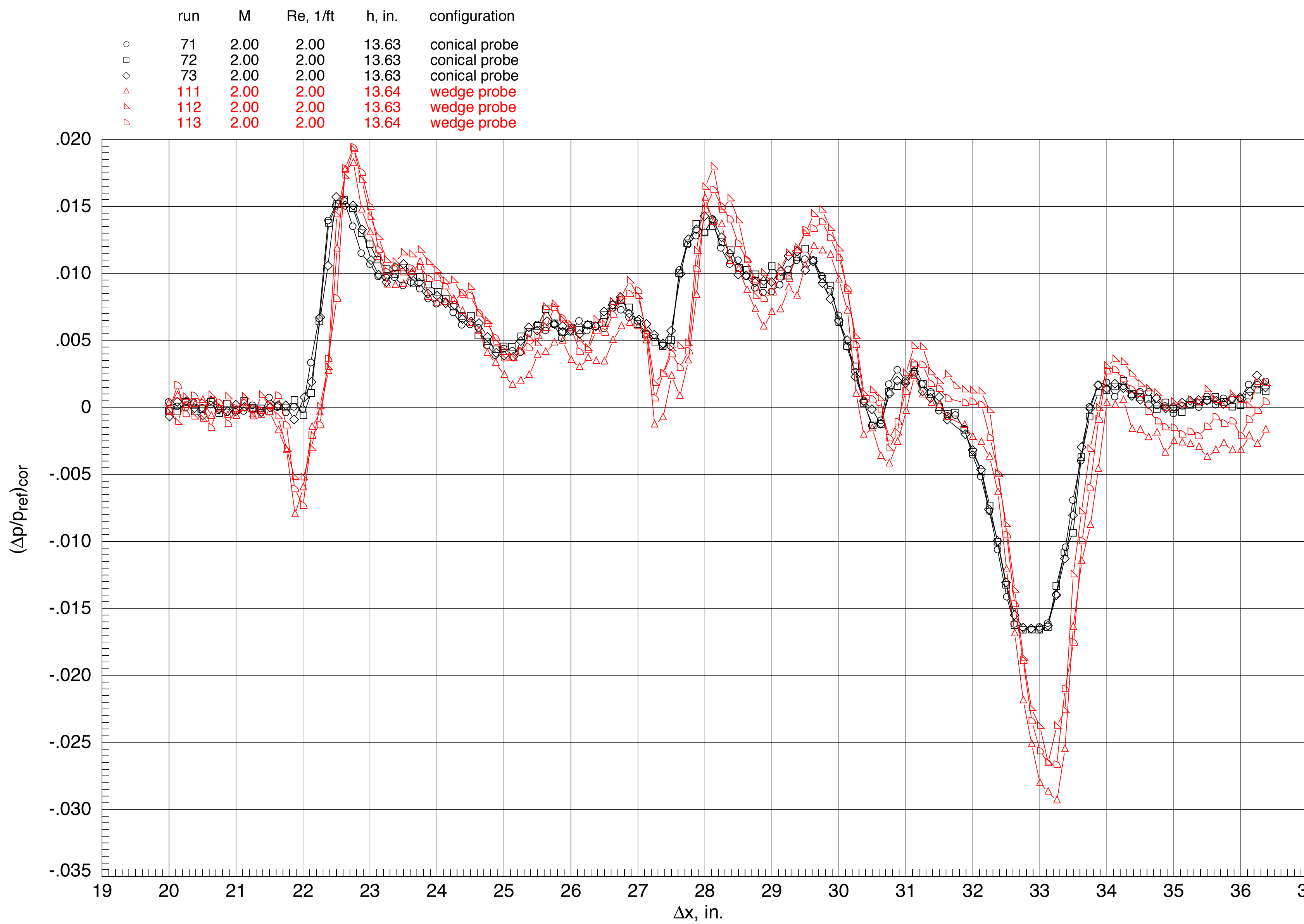

(b) Second set of repeats.

Figure 16. Concluded.

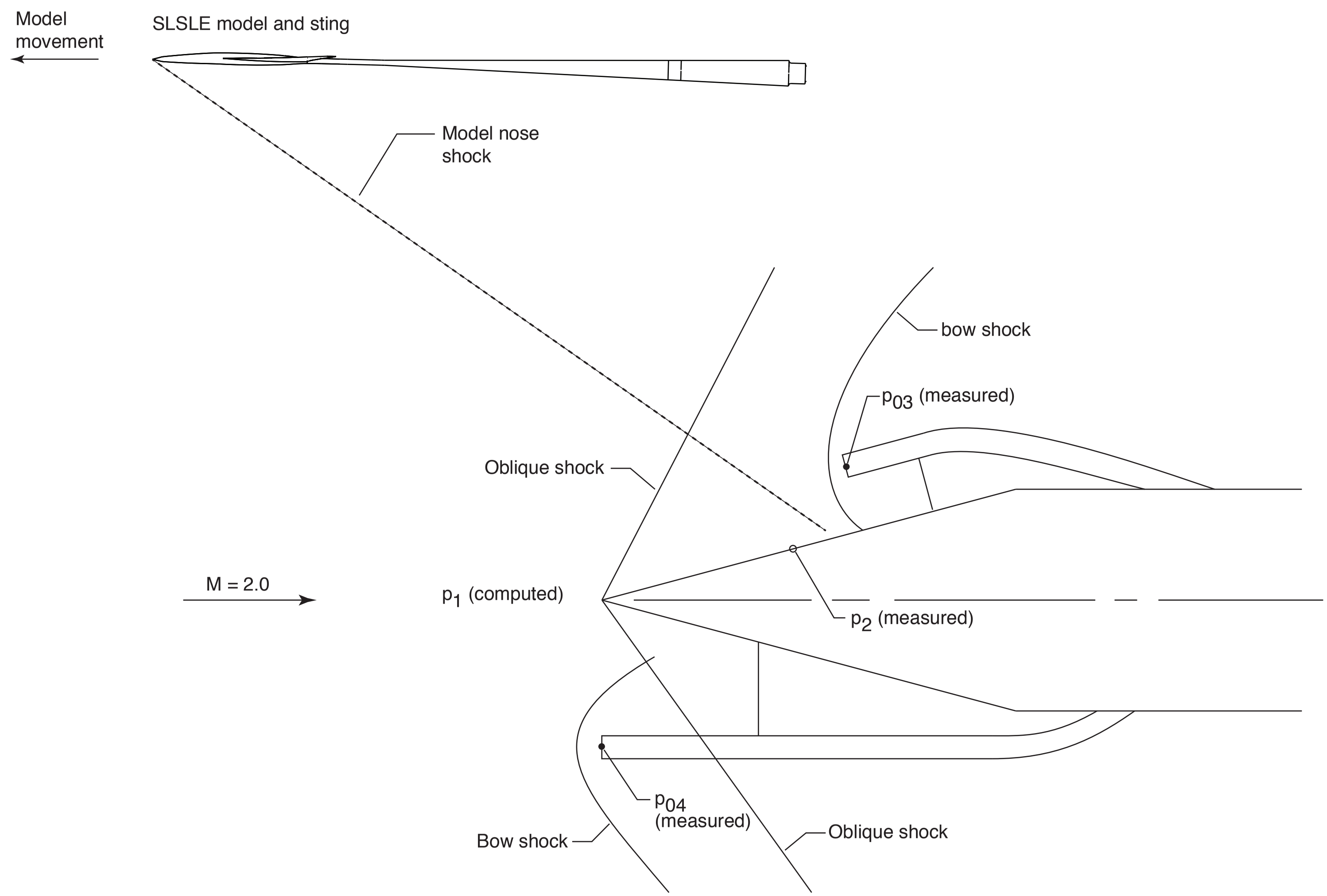

Figure 17. Sketch illustrating interaction of model nose shock and wedge probe.

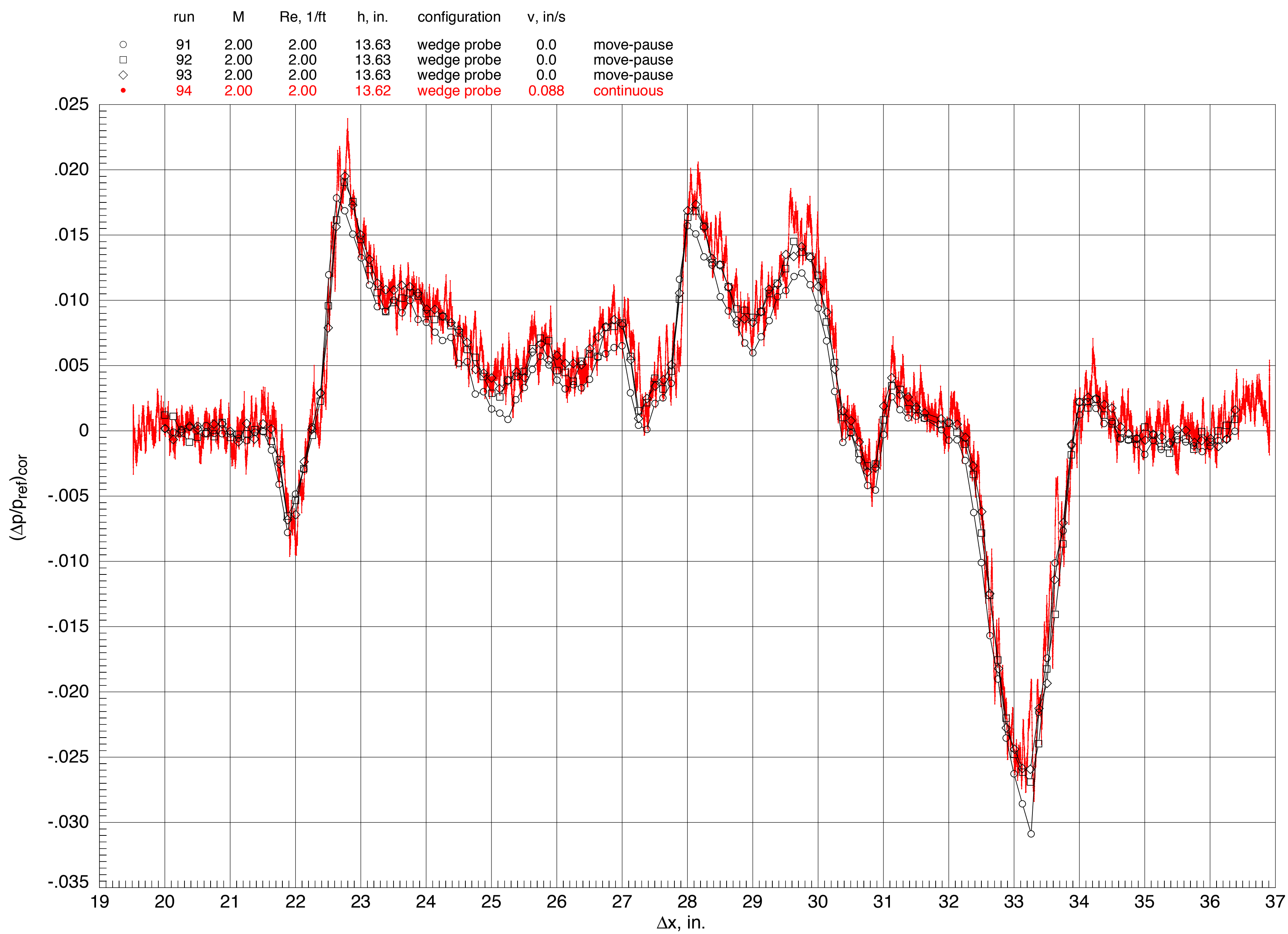

Figure 18. Comparison of wedge probe move-pause and continuous pressure signatures.

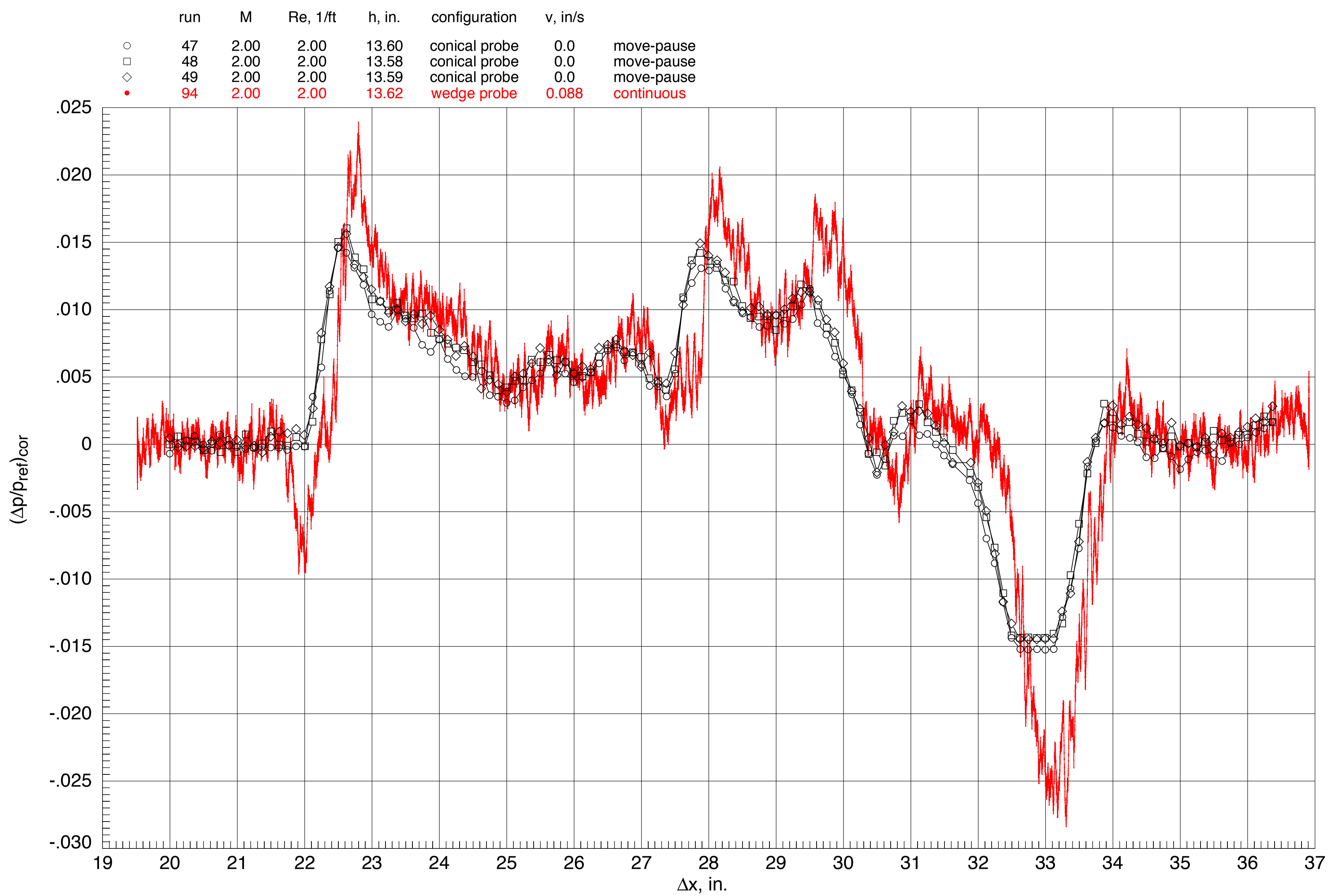

Figure 19. Comparison of conical probe move-pause pressure signatures and wedge probe continuous pressure signature.

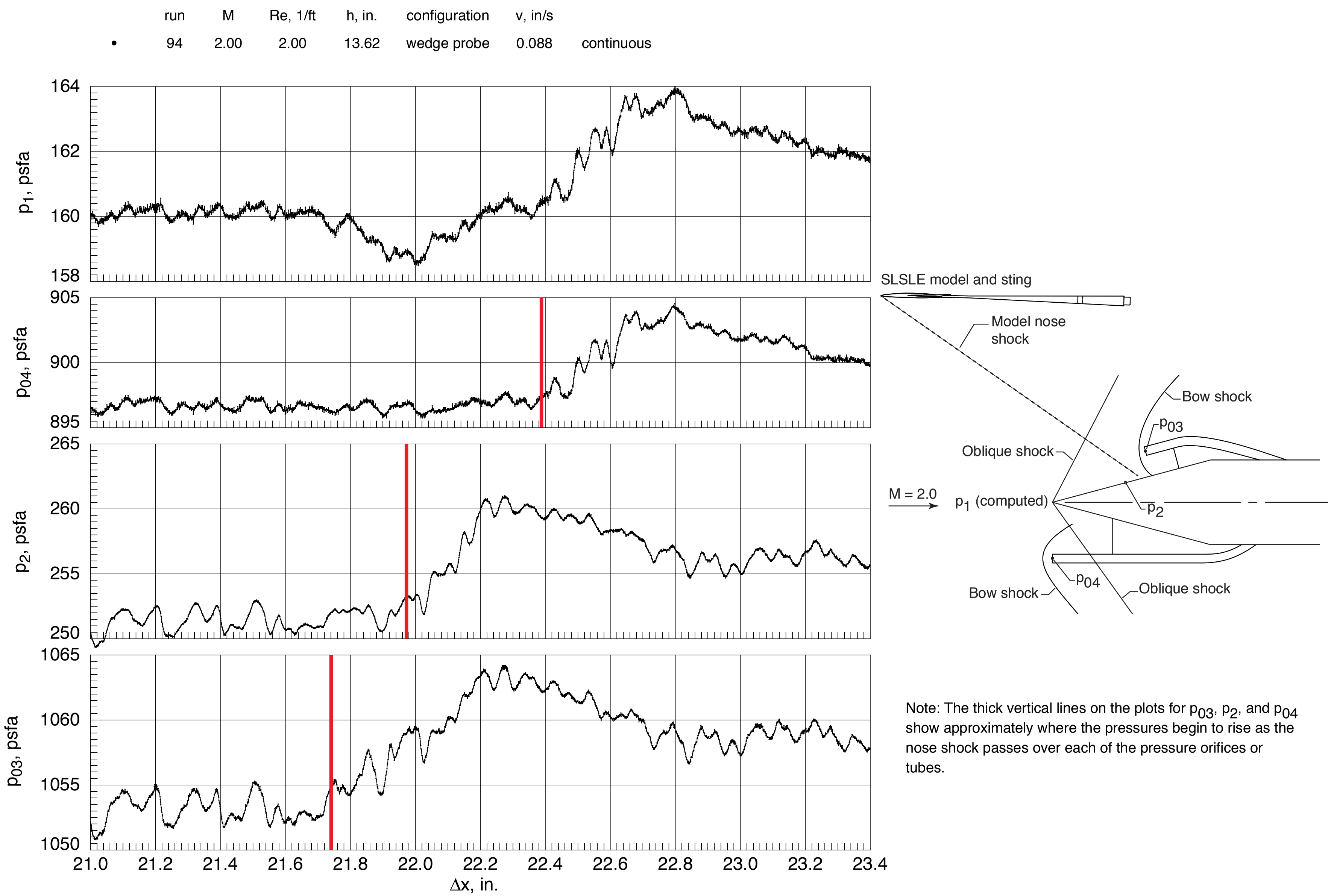

Figure 20. Wedge probe individual pressures measured during a continuous sweep run.

Appendix

Wedge Probe Data Reduction Procedure

The procedure used to reduce the data from the wedge probe is presented in this appendix. The procedure is based on the method documented in references 10 and 11. Figure A1 shows a sketch of the wedge and the nomenclature used in the equations. The pressures p_{03}, p_{04}, and p_2 were measured. These pressures and the known half angle of the wedge were used in an iterative procedure to compute the remaining variables listed in figure A1. The equations were derived for air with $\gamma = 1.4$.

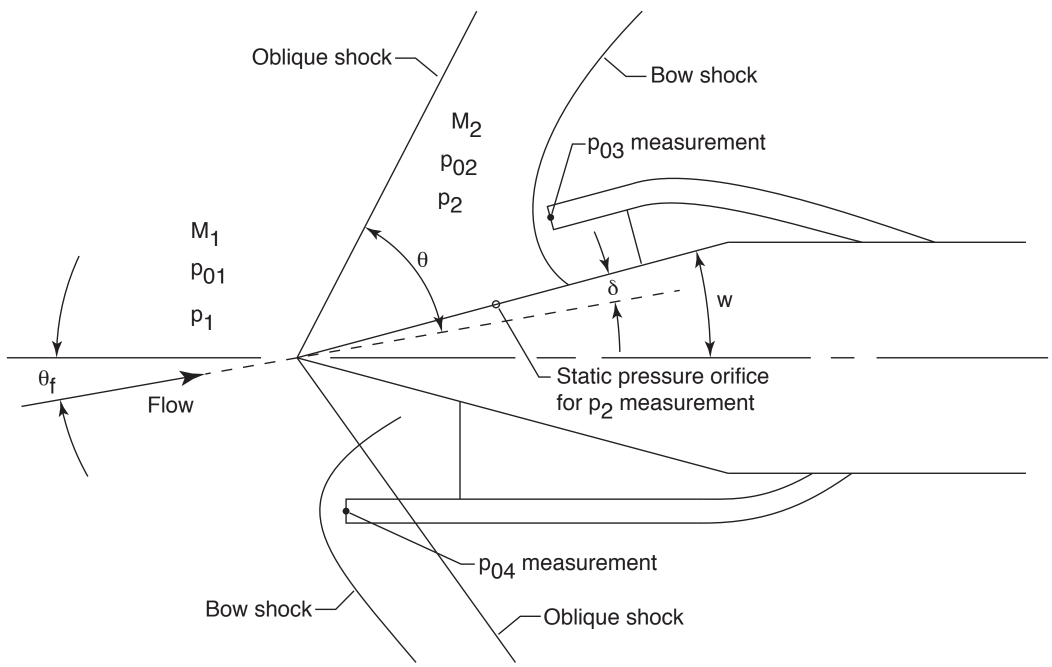

Figure A1. Sketch of wedge probe with nomenclature identified.

The following variables are measured or known:

p_2	measured static pressure on wedge upper surface, psfa
p_{03}	measured stagnation pressure behind normal shock on wedge upper surface, psfa
p_{04}	measured stagnation pressure ahead of wedge oblique shock and behind normal shock, psfa
w	wedge half angle (8° for wedge probe)

Using the above measured or known values in the procedure below results in the following computed values:

M_1	Mach number ahead of wedge probe
M_2	Mach number behind the wedge upper surface oblique shock
p_{01}	stagnation pressure ahead of wedge probe, psfa
p_{02}	stagnation pressure on wedge upper surface, psfa
p_1	static pressure ahead of wedge probe, psfa
δ	wedge upper surface flow deflection angle, deg
θ	wedge upper surface oblique shock wave angle relative to oncoming flow, deg
θ_f	flow inclination ahead of wedge probe (θ_f positive as shown in figure A1), deg

1. Compute estimate of M_2.

$$M_2 = \sqrt{\left(\frac{p_{03}}{p_2}\right)\left(\frac{35}{36}\right)^{5/2}\left(\frac{5}{6}\right)}$$

2. Compute p_{03}/p_2 using estimate of M_2.

$$\frac{p_{03}}{p_2} = \frac{(6)^6 M_2^7}{(5)^{7/2}(7M_2^2 - 1)^{5/2}}$$

3. Compute error between measured and calculated p_{03}/p_2.

$$error1 = \frac{\left(\frac{p_{03}}{p_2}\right)_{measured} - \left(\frac{p_{03}}{p_2}\right)_{calculated}}{\left(\frac{p_{03}}{p_2}\right)_{measured}}$$

4. Determine if the absolute value of $error1$ is greater than 0.0001.

$$|error1| > 0.0001$$

   If yes, then continue with step 5. If no, then continue with step 6.

5. Compute new estimate of M_2.

$$M_2 = M_2(1 + error1)$$

   Continue with step 2.

6. Compute p_{02}.

$$p_{02} = p_2\left(\frac{M_2^2 + 5}{5}\right)^{7/2}$$

7. Compute estimate of M_1.

$$M_1 = 72 - \sqrt{5161.538 - 153.846 M_2}$$

8. Compute estimate of $\xi = p_2/p_1$.

$$\xi = 1.41625 - 0.04M_1 + 0.055M_1^2$$

9. Compute Mach number ahead of wedge probe, M_1, squared.

$$M_1^2 = \frac{5\xi(\xi + 6)}{(6\xi + 1)}\left(\frac{p_{02}}{p_2}\right)^{2/7} - 5$$

10. Compute p_2/p_{04}.

$$\frac{p_2}{p_{04}} = \frac{5\xi}{6M_1^2}\left(\frac{35M_1^2 - 5}{36M_1^2}\right)^{5/2}$$

11. Compute error between measured and calculated p_2/p_{04}.

$$error2 = \frac{\left(\frac{p_2}{p_{04}}\right)_{measured} - \left(\frac{p_2}{p_{04}}\right)_{calculated}}{\left(\frac{p_2}{p_{04}}\right)_{measured}}$$

12. Determine if the absolute value of $error2$ is greater than 0.0001.

$$|error2| > 0.0001$$

If yes, then continue with step 13. If no, then continue with step 14.

13. Compute new estimate of ξ.

$$\xi = \xi(1 + error2)$$

Continue with step 9.

14. Compute p_1.

$$p_1 = \frac{p_2}{\xi}$$

15. Compute M_1.

$$M_1 = \sqrt{M_1^2}$$

16. Compute p_{01}.

$$p_{01} = p_1(1 + 0.2M_1^2)^{7/2}$$

17. Compute shock wave angle, θ.

$$\theta = \arcsin\sqrt{\frac{6\xi + 1}{7M_1^2}}$$

18. Compute flow deflection angle, δ.

$$\delta = \theta - \arcsin\sqrt{\frac{\xi + 6}{7\xi M_2^2}}$$

19. Compute flow inclination, θ_f.

$$\theta_f = w - \delta$$

20. Compute uncorrected sonic boom pressure signature parameter.

$$(\Delta p/p_{ref})_{unc} = \frac{p_1 - p_{ref}}{p_{ref}}$$

REPORT DOCUMENTATION PAGE

Form Approved OMB No. 0704–0188

1. REPORT DATE *(DD-MM-YYYY)*	2. REPORT TYPE	3. DATES COVERED *(From – To)*
01–08–2013	Technical Publication	

4. TITLE AND SUBTITLE
Effectiveness of a Wedge Probe to Measure Sonic Boom Signatures in a Supersonic Wind Tunnel

5a. CONTRACT NUMBER

5b. GRANT NUMBER

5c. PROGRAM ELEMENT NUMBER

6. AUTHOR(S)
Wilcox, Floyd J., Jr.; Elmiligui, Alaa A.

5d. PROJECT NUMBER

5e. TASK NUMBER

5f. WORK UNIT NUMBER
122711.03.07.07.16.80

7. PERFORMING ORGANIZATION NAME(S) AND ADDRESS(ES)
NASA Langley Research Center
Hampton, VA 23681–2199

8. PERFORMING ORGANIZATION REPORT NUMBER
L-20239

9. SPONSORING/MONITORING AGENCY NAME(S) AND ADDRESS(ES)
National Aeronautics and Space Administration
Washington, DC 20546–0001

10. SPONSOR/MONITOR'S ACRONYM(S)
NASA

11. SPONSOR/MONITOR'S REPORT NUMBER(S)
NASA/TP–2013–218036

12. DISTRIBUTION/AVAILABILITY STATEMENT
Unclassified - Unlimited
Subject Category 02
Availability: NASA CASI (443) 757-5802

13. SUPPLEMENTARY NOTES

14. ABSTRACT
A wind tunnel investigation was conducted in the Langley Unitary Plan Wind Tunnel (UPWT) to determine the effectiveness of a wedge probe to measure sonic boom pressure signatures compared to a slender conical probe. A generic business jet model at a constant angle of attack and at a single model to probe separation distance was used to generate a sonic boom signature. Pressure signature data were acquired with both the wedge probe and a slender conical probe for comparison. The test was conducted at a Mach number of 2.0 and a free-stream unit Reynolds number of 2 million per foot. The results showed that the wedge probe was not effective in measuring the sonic boom pressure signature of the aircraft model in the supersonic wind tunnel. Data plots and a discussion of the results are presented. No tabulated data or flow visualization photographs are included.

15. SUBJECT TERMS
Sonic boom; Aerodynamics; Supersonic; Wind tunnel test; Continuous data acquisition

16. SECURITY CLASSIFICATION OF: a. REPORT	b. ABSTRACT	c. THIS PAGE	17. LIMITATION OF ABSTRACT	18. NUMBER OF PAGES	19a. NAME OF RESPONSIBLE PERSON
					STI Help Desk (email: help@sti.nasa.gov)
					19b. TELEPHONE NUMBER *(Include area code)*
U	U	U	UU	50	(443) 757-5802

Standard Form 298 (Rev. 8/98)
Prescribed by ANSI Std. Z39.18